Studies on Metabolically Stable Compounds to Elucidate the Physiological Functions

A Dissertation Submitted to
the Graduate School of Life and Environmental Sciences,
the University of Tsukuba
in Partial Fulfillment of the Requirements
for the Degree of Doctor of Philosophy in Biological Science
(Doctoral Program in Biological Sciences)

Tomoko SATOMI

Table of Contents

Abstract

The research on metabolically stable compounds makes it possible not only to clarify various life phenomena, but also to utilize more stable compounds which are useful for various research of life sciences. In this thesis, I investigated metabolically stable compounds through kinetics and biochemical analysis.

In chapter 1, I investigated metabolic process of S-nitrosocysteine, which is one of endogenous S-nitrosothiols well known as an NO donor. Kinetics study revealed that S-nitrosocysteine had much longer half-life than NO in the presence of cysteine, which mimics a physiological condition. This result indicated that low-molecular-weight S-nitrosothiols, such as S-nitrosocysteine, could play a role as a sustainable NO donor *in vivo*, implying that S-nitrosothiols were the most suitable NO-generating agents for useful research tools but also possessed a potential for treatment of cardiovascular diseases. In chapter 2, I characterized the difference between M1 and M2-polarized macrophages using two types of metabolically stable chemical probes, 2-fluoro-2-deoxy-D-glucose (FDG) and ultrasmall superparamagnetic iron oxide (USPIO) particles. FDG and USPIO were useful clinical imaging agents for atherosclerosis. The analyses of intracellular accumulation of these chemical probes in human THP-1-derived macrophages indicated that M1-polarized inflammatory macrophages preferentially accumulated FDG than USPIO, due to upregulation of both glucose uptake and phosphorylation in M1 macrophages. This result suggested that FDG can be more useful than USPIO as an imaging probe that detects the M1-polarized inflammatory macrophages, which promote destabilization of plaques.

In summary, metabolically stable compounds are effectively useful as tools for not only investigating life phenomena, but also making diagnosis with a profound biological understanding of disease.

Abbreviations

CCR7	CC chemokine receptor7
CD	cluster of differentiation
Cys-SH	cysteine
Cys-SNO	S-nitrosocysteine
FDG	2-fluoro-2-deoxy-D-glucose
FPN1	ferroportin 1
FTL	ferritin light chain
GLUT	glucose transporter
G6P	glucose-6-phosphate
G6Pase	glucose-6-phosphatase
hIFNγ	human interferon-γ
hIL	human interleukin
HK	hexokinase
iNOS	inducible nitric oxide synthase
LPS	lipopolysaccharide
MRC1	mannose receptor, C type 1
MRI	magnetic resonance imaging
NO	nitric oxide
PET	positron emission tomography
PMA	phorbol 12-myristate 13-acetate
SR-A	scavenger receptor A
USPIO	ultrasmall superparamagnetic iron oxide particles

General Introduction

In all living organisms, including human, complex biochemical reactions are strictly regulated for sustainability of a life. Metabolism is one of the most important body regulation systems and comprises of several biochemical reactions (Newsholme EA, 1973; Martin BR et al., 1987). There are mainly three types of essential metabolic reactions, anabolism, catabolism and detoxification. Anabolism is a construction process of large molecules from smaller units, while catabolism is a break down process from large molecules into smaller subunits to generate energy. Similar to catabolism, another type of break down process in a higher organism is digestion which promotes absorption and assimilation of substances into a body (McGilvery, RW et al., 1983; Abeles RH et al., 1992). In general, a living organism takes substances from outside, and metabolizes it to generate energy in the form of ATP or to produce parts of cellular components. The metabolites were produced by the degradation process of large molecules – carbohydrate, protein and fat – taken as a nutrient, and convert into different form of cellular/body components. The components was used as a structure of a body, or preserved as an energy, and utilized it for life activities. Substance and energy exchanges ceaselessly between outside and inside of a body. This process is essential not only for maintenance of a body but also for power generation. Detoxification is an inactivation reaction of toxic substances derived from both endogenous and exogenous origins (Wanders RJ, 2013). Moreover, many other biochemical reactions related to metabolic pathway, such as signal transduction, contribute to the sustainability of living creatures. Various biochemical reactions associated with a metabolism continues as long as they are alive, reacting constantly against external environment changes. In this way, the living organisms have

an essential system called “homeostasis”, which maintains static condition of a body as a macro level by the active biochemical reactions as a micro level, in other words, dynamic equilibrium.

Dynamic equilibrium is a balance and flow of building block of a body; not only an exchange of cellular components but also food intake contribute to the homeostasis (Schoenheimer R, 1946). Glucose metabolism is a typical example of physiological regulation of metabolic status. Food-derived carbohydrates, such as sucrose and starches, are enzymatically digested to origo- and mono-saccharide, including glucose, and then absorbed into a small intestine and dispersed throughout a body via blood stream. Glucose is used to generate energy, as a form of ATP, by both glycolysis and tricarboxylic acid (TCA) cycle in several tissues. Moreover, excess mount of glucose is stored as glycogen in liver or as lipids in fat. Glucose is so important, as an energy source of every organ. Several feedback systems strictly regulate plasma glucose level. Significantly low plasma glucose level called hypoglycemia causes disruption of brain function due to a lack of energy supply, resulting in severe symptoms such as seizure, consciousness disturbance and lethargy. On the other hand, chronic high blood glucose level called hyperglycemia damages several tissues due to an accumulation of protein modifications by glucose itself. Insulin is a hormone produced by ß-cells in the pancreas, regulating the metabolism of carbohydrates by sensing plasma glucose level. Insulin activates absorption of glucose into skeletal muscles and fat tissue, and accelerated intracellular glucose metabolisms such as glycolysis and lipid biosynthesis as well. Similar to carbohydrate, food-derived protein is also digested to amino acids in an intestine, and

then absorbed into a body. The absorbed amino acids are transferred to liver through blood capillary and portal vein. A part of these amino acids is reused for protein biosynthesis; especially food-derived essential amino acids are important sources of proteins synthesis in a body. The other portion of amino acids is metabolized. The first step of the amino acid metabolism is a removal of amino group, which is becomes ammonium ion, and then incorporated into Urea cycle, and finally excreted from a kidney as a form of urea. After removal of amino group, the carbon skeleton is further metabolized to organic acids, some of which are introduced into energy generation cycle, such as TCA cycle, or are used for biosynthesis of glucose (gluconeogenesis) and ketone body as the other form of energy. Cellular amino acid level is maintained at a same level by mixing with food-derived amino acids and body protein derived amino acids, which is called Amino acid pool. Imbalance of amino acid pool sometimes cause imbalance of a body function because amino acid plays multiple roles by transforming to both energy sources and building block of a cell, such as protein and lipid. Lipid derived from food components and *de novo* biosynthesis process distributed in different forms, such as phospholipid and acylglycerol. Phospholipid is main component of cellular/subcellular membrane. Acylglycerol, especially triacylglyerol, is stored in adipose tissues as a form of energy storage. When supply of glucose is restricted like starvation condition, amino acid and lipid become alternative sources of energy. Free fatty acids hydrolyzed from triacylglycerol distribute to several parts of body via blood flow. In cells, the free fatty acid is incorporated into mitochondria, and decomposed by ß-oxidation pathway to generate

energy. The dynamic metabolism of carbohydrate, protein and lipid contribute to the main part of homeostasis, determining physical condition of a body.

Meanwhile, local and transient reactions, such as acute protective response and signal transduction, are also indispensable systems of life. Nitric oxide (NO) is a signaling molecule, synthesized by an enzyme called NO synthase. NO transmits various biological signals in variety of cells and tissues, such as regulation of blood flow, neurotransmission, and mediation of immunological responses (Bredt DS, 1994). NO functions locally and promptly since NO is immediately disappears due to the instability. Body protection system is another example of acute reaction. For example, acute inflammatory response locally occurs immediately after an infection of virus or microorganisms, and gradually goes into a suppressive immunization process with the decline of the external stimuli (Levy JH, 1996). Inflammatory response is one of the most complex biological processes by various biochemical substances in different types of cells. This system is too complicated to figure out the whole picture yet.

Various chemical reactions constantly happen *in vivo*. Clarifying a mechanism of biochemical reactions and its complicate combination in a body is a critical issue of biochemistry and biology research. Chemical kinetics becomes a strong tool to elucidate a mechanism of biological reactions in molecular level. A major player in biological reaction is enzyme, whose diversity is significant and contribute to almost all chemical alteration in a body. Therefore, enzymatic kinetics research could reveal not only the enzymatic machinery the activity regulation, but also boost a biology research and a drug development. Theoretically, uncovering reaction-rate-equation of every enzyme in a

biological system could reveal all rate-constants that decide speeds of every reaction, which could unveil entire biological system (Cook PF et al., 2007). A precise understanding of respective reactions requires a simplified system focusing on each biological reaction, although sophisticated biological systems is established with an elaborated of individual reactions; large number of intermediates and the sub-reactions and reverse reactions makes the physiology complicated.

Enzymatic reaction experiments are performed by using a recombinant enzyme; concentration monitoring of substrates and products can reveal the kinetics of the enzyme. This is a most simplified experiment for enzymatic reaction, but often difficult to estimate actual function in a complex biological system because of the complex molecular/cellular/tissue interactions. Popular approach to investigate the real function of an enzyme in a body is a tracer experiment. For example, after adding isotope-labeled glucose, such as ^{13}C-labeled or ^{14}C-labeled, in cells/tissues, monitoring concentration change of isotope-labeled glucose and generation of isotope-labeled glucose metabolites could clarify the fate and kinetics of glucose metabolism in a biological system. In this type of study, nucleic magnetic resonance spectroscopy (NMR) and mass spectrometry (MS) play a powerful role to monitor labeled molecules. As for *in vivo* molecular kinetics research, molecular imaging modalities – positron emission tomography (PET), single-photon emission computed tomography (SPECT), functional magnetic resonance imaging (fMRI) – are able to monitor dynamic flow of labeled- or endogenous molecules (Osborn EA et al., 2013). [^{18}F]-2-fluoro-2-deoxy-D-glucose (^{18}F-FDG) PET is often used for detection of tumor because of the active glucose uptake (flow) in cancer cells (Smith TA,

1998), and for studying glucose utilization (kinetics) in several tissues as well. Hence, imaging technologies and high sensitive molecular probes that visualize the specific molecular pathway in a body have become valuable tools for several life science fields.

In this thesis, I investigated the usefulness of metabolically stable compounds, such as S-nitrosocysteine, FDG, and USPIO, as tools for various biological approaches. In Chapter 1, the decomposition kinetics of S-nitrosocysteine, one of endogenous S-nitrosothiols, were investigated in order to understand its usefulness as a sustainable NO donor. I discussed the physiological role and usefulness of S-nitrosocysteine and the future perspective to its clinical translation, led by my study. In Chapter 2, M1/M2-polarized macrophages were characterized using two types of chemical probes, FDG and USPIO, which were metabolized through different pathways. Biological readout of the imaging using FDG and USPIO in atherosclerosis was discussed based on kinetic research of these compounds in the different type of macrophages. I also discussed the results from the point of view of translational research.

Chapter 1

Kinetic Studies on the Reaction of S-nitroso-L-cysteine with L-cysteine

Abstract

Kinetics for the reaction of S-nitroso-L-cysteine (S-nitrosocysteine) decomposition in the presence of L-cysteine (cysteine) were examined in a physiological condition, with an aim to find out if S-nitrosothiols have stability to reserve and transport nitric oxide (NO) in a body. Rates for the reaction between S-nitrosocysteine and cysteine were found to be first order with respect to concentrations of the two reactants in the pH range of 4.85 - 9.41. The second order rate constant was determined to be 3.10×10^{-2} $M^{-1}s^{-1}$ at pH7.4 at 37°C. Spontaneous decomposition of S-nitrosocysteine proceeded with the first order rate constant, 1.46×10^{-5} s^{-1} under the same conditions. These rate constants for the decomposition of S-nitrosocysteine as one of endogenous S-nitrosothiols in the presence of cysteine at pH7.4 at 37°C leaded to estimate the half-life of S-nitrosocysteine in a physiological condition. The half-life of S-nitrosocysteine was calculated to be 75 min based on the k_2 value in the presence of cysteine under this experimental condition, and was much longer than NO. This kinetic result suggests that S-nitrosocysteine stability is sufficient to function as a reservoir and transporter of NO in physiological environments, such as blood and cytosol.

Introduction

Nitric oxide (NO) is a biological messenger molecule produced in mammals via the oxidation of L-arginine to citrulline by NO synthase, which NO is observed in a wide variety of cell types, including macrophages, vascular endothelial cells, neurons, epithelial cells, and neutrophils (Marletta MA, 1993). For example, soluble guanylate cyclase contains heme as a prosthetic group, and is activated up to 200-fold increase in catalytic rate, i.e. the conversion of GTP to cyclic guanosine monophosphate (cGMP) by the binding of NO to that heme (Derbyshire ER et al., 2009). In blood vessels, cGMP as a second messenger induces relaxation of vascular smooth muscles and inhibition of platelet aggregation leading to vasodilation and increased blood flow. NO was identified as endothelium-derived relaxing factor (EDRF) (Ignarro LJ, 1989; Ignarro LJ et al., 1987; Palmer RMJ et al., 1987; Furchgott RF, 1988; Feelisch M et al., 1994), but S-nitrosothiols had also been considered to be one of most plausible candidates for EDRF in times past (Ignarro LJ, 1989). Meanwhile, the accumulated observations, as indicated by the following examples, suggest that NO is reserved and transported as nitrosothiols, the carriers, which then give their NO to metal prosthetic groups or cysteine residues of the target proteins to transduce signaling: (a) NO reacts readily with thiols to give the corresponding S-nitrosothiols (reaction 1) (Stamler JS et al., 1992[p1]; Stamler JS et al., 1992[s]; Stamler JS et al., 1992[p2]; Girard P et al., 1993; Rand MJ et al., 1995). (b) S-nitrosothiols are much more stable than NO, which is a labile free radical with the biological half-life of several seconds. Cys-34 residue of serum albumin is nitrosylated to

form long-lived S-nitrosoalbumin which may act as a reservoir and carrier of NO in plasma (Simon DI et al., 1993; Shcarftein JS et al., 1994). (c) Thiols potentiate the action of NO. For example, relaxant action of NO on the rat anococcygeus muscle is much greater and more prolonged in the presence of cysteine (Cys-SH) than in its absence (Rand MJ et al., 1995). S-nitrosocysteine (Cys-SNO) is a more potent relaxant of endothelium-denuded strips of rabbit aorta than NO. S-nitrosothiols provide NO to soluble guanylate cyclase (Feelisch M et al., 1994). The NO binding to the heme moiety of the guanylate cyclase triggers the generation of cyclic GMP, the next messenger in the NO-mediated signaling pathway. (d) Nitroso group transfer, transnitrosation (reaction 3) between S-nitrosothiols and thiols takes place readily (Shcarftein JS et al., 1994; Arnelle DR et al., 1995; Barnett DJ et al., 1994; Barnett DJ et al., 1995). (e) S-nitrosation of cysteine residues of the particular proteins modulates their functions (Jia L et al., 1996; Hajjar DP et al., 1995; Gross WL et al., 1996; Mohr S et al., 1994; Stamler JS, 1994).

$$\text{R-SH} + \text{NO} \rightarrow \text{R-SNO} + \text{H}^+ + \text{e}^- \quad (1)$$

$$\text{R-SNO} \rightarrow 1/2\ \text{R-S-S-R} + \text{NO} \quad (2)$$

$$\text{R-SNO} + \text{R'-SH} \rightarrow \text{R-SH} + \text{R'-SNO} \quad (3)$$

$$\text{R-SNO} + \text{R'-SH} \rightarrow \text{R-S-S-R'} + \text{HNO} \quad (4)$$

Since all physiological events are rate processes, understanding the biological roles of S-nitrosothiols requires rates and mechanisms of the key reactions 1-4 in regard to S-nitrosothiols. The kinetics data and mechanisms for the Cys-SNO-forming reaction of

NO with cysteine (reaction 1) were previously reported by two groups (Kharitonov VG et al., 1995; Goldstein S et al., 1996). When the reaction 1 is carried out under aerobic conditions, oxygen molecule acts as the electron acceptor (Kharitonov VG et al., 1995; Goldstein S et al., 1996). Kinetic studies on the transition metal ion-catalyzed NO-regenerating process from S-nitrosothiols (reaction 2) were investigated by Williams et al. (McAninly JJ et al., 1993; Askew SC et al., 1995). Arnelle and Stamler showed in their *in vitro* semi-quantitative studies of the reaction 2 that the apparent life times of S-nitrosothiols vary depending on the analytical methods (Arnelle DR et al., 1995). The kinetics and mechanisms of the transnitrosation from S-nitrosothiols to thiols (reaction 3) were extensively studied by Williams and coworkers (Barnett DJ et al., 1994; Barnett DJ et al., 1995).

In this way, although thiols produce S-nitrosothiols in biological systems, they also destroy S-nitrosothiols to give disulfides (reaction 4) as reported by Oae et al (Oae S et al., 1977). On the contrary, Feelisch et al. reported that the life-time of Cys-NO is prolonged by the presence of cysteine in a concentration-dependent manner (Feelisch M et al., 1994). Since the thiol concentration level in normal living cells is pretty high (ca. 5 mM) (Schultz et al., 1979), the decomposition reaction of S-nitrosothiols with thiols (reaction 4) is of importance but its kinetics study has not as yet been reported. Thus, I conducted the kinetic studies of the decomposition reaction of Cys-SNO in the presence and absence of Cys-SH to solve these problems.

Materials and Methods

Preparation of Cys-SNO

L-cysteine (cysteine, Cys-SH) was allowed to react with an equimolar amount of nitrous acid in an aqueous solution of pH 1-2 for 3 min at room temperature. The pH of the solution was raised to 7 by adding a NaOH solution quickly. The solution of S-nitroso-L-cysteine (S-nitrosocysteine, Cys-SNO) was treated with Chelex 100 ion exchange resin (Bio-Rad) on ice to remove any trace heavy metal ions which might be contained in the solution. Buffer solutions and Cys-SH solution were also treated with Chelex 100 ion exchange resin, since heavy metal ions, especially Cu^{+}, catalyze the decomposition of nitrosothiols as noted by Williams et al (McAninly JJ et al., 1993; Askew SC et al., 1995). All the solutions contained 0.1 mM ethylendiaminetetraacetate (EDTA) to protect Cys-SNO from the heavy metal catalyzed decomposition. The solution of Cys-SNO thus prepared is stable for a few days on ice and is stored protected from light.

$$\text{Cys-SH} + \text{HONO} \rightarrow \text{Cys-SNO} + H_2O \qquad (5)$$

Molar Extinction Coefficient of Cys-SNO

Equimolar amounts of known concentration of Cys-SH in 0.1 M HCl solution and aqueous sodium nitrite ($NaNO_2$) solution were mixed in a quartz UV cuvette and the increasing absorbance at 543 nm was recorded. After 3 min the absorbance reached to plateau. The value of e was calculated from the maximum absorbance of 852 $M^{-1}cm^{-1}$

(λmax 335 nm) and 16.8 $M^{-1}cm^{-1}$ (λmax 543 nm) by assuming that Cys-SH was converted to Cys-SNO quantitatively. The experiment was repeated 3 times and was reproducible. The same value was obtained under argon atmosphere.

Absorbance Determination of Cys-SNO

UV-visible spectra of Cys-SNO were recorded on a JASCO Ubest-50 spectrophotometer equipped with a quartz UV cuvette with a water jacket to which water of 37 ± 0.1°C was circulated from a NESLAB RTE-210 refrigerated bath. When a microsyringe with a stainless steel needle and piston to transfer Cys-SNO into a UV cuvette was used, metal ion catalyzed decomposition of Cys-SNO took place rapidly at an unreproducible rate. Therefore, these solutions were pipetted by an eppendorf-pipette. All the pH values were measured at 37°C by Horiba M-13 pH meter. The following buffer solutions were used: pH5-6, sodium acetate; pH6-8, sodium phosphate; pH8-9, sodium borate.

Results

Since most of thiols contained in peptides and proteins come from cysteine residues, kinetics of the reaction of Cys-SNO with Cys-SH (reaction 6) were studied. Both the nucleophilic substitutions on the nitroso-nitrogen (reaction 3) and on the sulfer (reaction 4) of an S-nitrosothiol with a thiol are orbital controlled reactions (Oae S et al., 1978; Klopman G et al., 1974) and therefore these reactions may occur smoothly. The reversible transnitrosation reaction 3 and the irreversible reaction 4 take place competitively (Arnelle DR et al., 1995). However, since R and R' are the same in this work, the reaction 3 does not interfere in the kinetic investigation of the reaction 6. Three fates await the HNO formed by the reaction 6, i.e. the condensation reaction 7 to give dinitrogen oxide, single electron oxidation affording NO (reaction 8) (Fukuto JM et al., 1993), and the reduction by thiol affording hydroxylamine (reaction 9) (Arnelle DR et al., 1995). In accordance with the observation by Arnelle and Stamler (Arnelle DR et al., 1995), no hydroxylamine was detected in the reaction mixture of Cys-SNO with Cys-SH, suggesting that HNO disappears via the reactions 7 and 8.

$$\text{Cys-SNO} + \text{Cys-SH} \rightarrow \text{Cys-S-S-Cys} + H^+ + NO^- \quad (6)$$

$$2\,NO^- + 2H^+ \rightarrow N_2O + H_2O \quad (\text{pKa of HNO} = 4.7) \quad (7)$$

$$NO^- + \text{ox} \rightarrow NO + \text{ox}^- \quad (8)$$

$$NO^- + 2\text{Cys-SH} + H^+ \rightarrow H_2NOH + \text{Cys-S-S-Cys} \quad (9)$$

$$\text{Cys-SNO} \rightarrow \text{Cys-S-S-Cys} + NO \quad (10)$$

The kinetic measurements of the reaction between Cys-SNO and Cys-SH were carried out by adding the Cys-SH solution to the Cys-SNO solution in the UV cuvette at 37.0°C and recording the absorbance of Cys-SNO at 335 nm or 543 nm. The rates were calculated from the slope of the time courses of the absorbance at the initial stage. When [Cys-SNO] was fixed to a value of 9.5 mM, the initial decay rates of Cys-SNO increased linearly with [Cys-SH] as shown in Fig. 1 (A). In the absence of Cys-SH the very slow unimolecular spontaneous decomposition of Cys-SNO proceeded with the first order rate constant (1.46 ± 0.08) x 10^{-5} s^{-1}. With a fixed [Cys-SH] of 24.5 mM, the initial rates of Cys-SNO decay correlated linearly with [Cys-SNO] as shown in Fig. 1 (B). From these observations, one obtains the rate equation 11.

$$V = k_1[\text{Cys-SNO}] + k_2[\text{Cys-SNO}][\text{Cys-SH}] \qquad (11)$$

The second order rate constants (k_2) were calculated from the slope of the line in Fig. 1 (A) to obtain (2.20 ± 0.07) x 10^{-2} $M^{-1}s^{-1}$. From eqn. 11, the slope of the line in Fig. 1 (B), (2.20 ± 0.03) x 10^{-2} $M^{-1}s^{-1}$, is equal to ($k_2 + k_1/[\text{Cys-SH}]$). Substituting k_1 and [Cys-SH] with 1.46 x 10^{-5} s^{-1} and 24.5 mM in this equation, one gets k_2 = 2.14 x 10^{-5} s^{-1}. The good agreement of the two k_2 values calculated based on the different kinetic data sources, *i.e.* Figure 1 (A) and 1 (B), substantiates that Cys-SNO disappears through the Cys-SH-induced bimolecular decomposition pathway (reaction 4) accompanied with minor Cys-SH-independent unimolecular decomposition process (reaction 2). The k_1 value was found to be independent of the pH of the solution.

The values of k_2 were determined in the pH range of 4.85-9.41 with the initial concentrations of the reactants to be [Cys-SNO] = 9 mM, [Cys-SH] = 24 mM and [buffer] = 0.1 M, respectively. The kinetic measurements were repeated 3-5 times for each condition. The k_2 values determined in the solutions of different pH values at physiological temperature are listed in Table 1 and the pH-rate profile is shown in Fig. 2. It was difficult to explain such a small pH-effect, namely, that maximum value of k_2 at pH 8.15 was merely 2 folds greater than the minimum one at pH4.85, although $[H^+]$ between the two differed by 2×10^3 folds.

Discussion

With respect to spontaneous unimolecular decomposition of Cys-SNO, based on k_1 = 1.46 x 10^{-5} s^{-1}, the half-life of Cys-SNO in the absence of cysteine was calculated to be approx. 9 hr at 37°C. This value was much greater than the half-life of Cys-SNO reported previously, *i.e.* the values of approx. 1.5 hr, as calculated from the Park's second order rate constant if $[Cys\text{-}SNO]_0$ = 10 mM (Park JW et al., 1988) and the values in the range of 1-2 hr, as room temperature as reported by Arnelle and Stamler (Arnelle DR et al., 1995). This discrepancy would be due to the effect of trace amounts of transition metal ions, which were very carefully eliminated in this work as described in Experimental Section. Thus, the k_1 value determined is the most reliable value for the uncatalyzed spontaneous decomposition of Cys-SNO. Such a small k_1 value reveals that the spontaneous NO release from S-nitrosothiols may not be responsible for the biological NO transfer from S-nitrosothiols to soluble guanylate cyclase. Instead, the transition metal ions-catalyzed NO-forming reaction of S-nitrosothiols and/or direct NO transfer from nitrosothiols to the guanylate cyclase via bimolecular reactions of the two species may operate in the biological NO transfer from the S-nitrosothiols to the guanylate cyclase. The uncatalyzed decomposition of Cys-SNO is too slow to explain the NO-transfer from an NO-carrying S-nitrosothiol to cysteine residues of the target proteins via reaction 2 followed by reaction 1. The transnitrosation (reaction 3) may be responsible for this S-nitrosothiol function.

Next, regarding Cys-SH-induced bimolecular decomposition of Cys-SNO, S-nitrosothiols are thought to play the same role as NO to control vasodilation and antiplatelet effects, and modulation of the reactivities of hemoglobin (Jia L et al., 1996), prostaglandin H synthase (Hajjar DP et al., 1995), creatine kinase (Gross WL et al., 1996), glyceraldehyde-3-phosphate dehydrogenase (Mohr S et al., 1996) etc. by the transnitrosation reaction 2 to the respective cysteine residues of these proteins. Especially, it has been postulated that S-nitrosohemoglobin, which protects and transports NO in red blood cells, dispenses NO bioactivity to microvascular cells on the release of oxygen, physiologically coupling hemoglobin deoxygenation to vasodilation (Crawford JH et al., 2003; Allen BW and Piantadosi CA, 2006; Angelo M et al., 2006). Recently, Tejero J *et al.* reported that reductive nitrosylation of hemoglobin was faster at low NO concentrations and sensitive to allosteric modifications, indicating that it might be more relevant *in vivo* than previously recognized (Tejero J et al., 2012). If these S-nitrosothiol-dependent reactions contribute in biological regulations, the S-nitrosothiol concentrations have to be greater than the threshold in a local compartment sending the signal. Usual mammalian cells contain about 5 mM of the reduced form of glutathione (Schultz GE et al., 1979). Assuming that reactivities of intracellular S-nitrosothiols and thiols are the same as those of Cys-SNO and Cys-SH at least in the case of low-molecular-weight thiols, the pseudo-first order rate constant for the decay of an intracellular S-nitrosothiol to be 1.55×10^{-4} s^{-1} at pH7.4, at 37°C from the k_2 value determined in this work was obtained. Under this condition, the half-life of an

S-nitrosothiol was calculated to be 75 min. If the rate of S-nitorosothiol formation is greater than 1.55×10^{-4} s^{-1}, the intracellular concentration of S-nitorosothiol will increase.

In my experiments, the presence of Cys-SH did not prolong the life-time of Cys-SNO but merely decrease it in concentration-dependent manner in contrary to the report by Feelish *et al* (Feelisch M et al., 1994). They tested the half-lives of various candidates containing Cys-SNO using the bioassay system comprised rabbit aortic strips, whereas I estimated its half-life by directly absorbance determination. The difference of experimental system might create this discrepancy. I would also like to mention that more recent kinetic studies on decomposition reaction between S-nitrosothiols and thiols by Hu *et al.* were also showed less effect on pH (Hu TM et al. 2006) along with my experimental results as a small pH-effect on k_2.

The apparent second order rate constants of transnitrosation reaction 3 are in the order of 10 $M^{-1}s^{-1}$ at pH7.4 (Barnett DJ et al., 1994; Barnett DJ et al., 1995). Therefore, in order that the S-nitrosation of the target protein with intracellular S-nitrosothiol (reaction 3) proceeds faster than the intracellular thiol dependent decomposition of the S-nitorosothiol (reaction 4), the concentration of the target protein should be greater than 10^{-5} M.

NO^- undergoes single electron oxidation with biological oxidant (even molecular oxygen) yielding NO. Fukuto *et al.* argued that NO^- was oxidized to NO (reaction 8) before binding to the guanylate cyclase. The guanylate cyclase requires ferrous nitrosylheme, $[PFe^{II}(NO)]$ (Craven PA et al., 1978), as a cofactor but not the ferric state. Hemin, $[PFe^{III}]$, may accept NO^- to generate $[PFe^{II}(NO)]$. Then the reaction 1, 2, 4, and 8 would contribute

partly and explain why Cys-SH prolongs and potentiates the vasodilation effect of NO and Cys-SNO.

Taken together, the present kinetic results suggest that the half-life of S-nitrosocysteine, which is one of endogenous S-nitrosothiols, is much longer than the half-life of NO in physiological environments. The fact that S-nitrosocysteine stability is sufficient to function as a reservoir and transporter of NO indicates S-nitrosothiols including S-nitrosocysteine should be able to use as an NO-generation reagent. Actually, some S-nitrosothiols are widely used for study on the physiological action of NO through to the present. Some S-nitrosothiols come into common use in life science research as stable NO donors, such as S-Nitroso-N-acetyl-DL-penicillamine (SNAP), S-nitrosoglutathione, and Cys-SNO. Especially, S-nitrosoglutathion, one of S-nitrosothiols, has also been used as an NO donor for treatment of patients in small clinical trials (Molloy J et al., 1998; Salas E et al., 1998; Rassaf T et al., 2002). S-nitrosoglutathione and Cys-SNO, which are derived from glutathione and cysteine existed widely in the body, are water-soluble and substantially play a role as physiologically active substance thought they are relatively unstable for practical purposes. SNAP is more stable than S-nitrosoglutathione and Cys-SNO but less soluble in water. The usage is selected from these S-nitrosothiols depending on the situation.

Various metabolically stable substances are widely used as tool compounds in elucidation of reaction mechanism caused by not only short-lived molecules but also metabolic substrates in a state of dynamic equilibrium. For example, [^{18}F]-2-fluoro-2-deoxy-D-glucose (^{18}F-FDG) is a glucose analogue widely used to study

tumor metabolism and inflammatory lesion by means of positron emission tomography (PET). Just as glucose, FDG is actively transported into the cell mediated by a group of structurally related glucose transporters (GLUT). Once intracellular, both glucose and FDG are phosphorylated by hexokinase as the first step toward glycolysis. FDG cannot be further metabolized to fructose-6-phosphate by glucose-phosphate-isomerase, so FDG remains trapped in the cell as FDG 6-phosphate. Additionally, another example of them is [^{123}I]-15-(*p*-iodophenyl)-3-(R,S)-methyl-pentadecanoic acid (^{123}I-BMIPP). BMIPP is a methyl-branched chain fatty acid analog used as a metabolic imaging agent suitable for myocardial single photon emission computed tomography (SPECT). BMIPP shows high accumulation as well as prolonged retention in the myocardium because it is eventually, after α-oxidation, oxidized by mitochondrial β-oxidation (Yoshinaga K et al., 2007). In chapter 2, using two types of metabolically stable chemical probes, 2-fluoro-2-deoxy-D-glucose (FDG) and ultrasmall superparamagnetic iron oxide (USPIO) particles, the difference between M1 and M2-polarized macrophages was characterized.

Figures and Table

Figure 1. Kinetic results for the decay of S-nitrosocysteine in the presence of cysteine at pH4.8 at 37°C. (A) Initial rate plot of Cys-SNO decomposition on Cys-SH concentration. (B) Initial rate plot of Cys-SNO decomposition on Cys-SNO concentration.

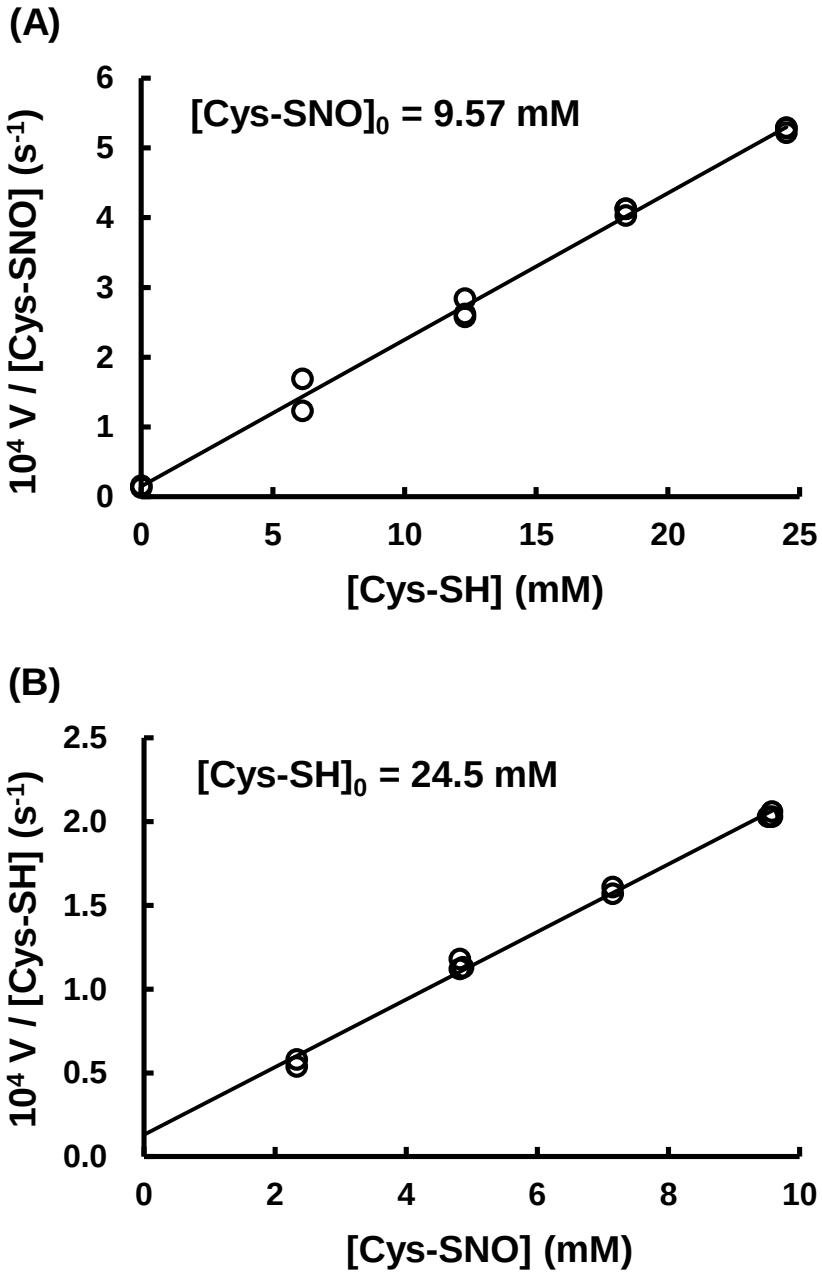

Figure 2. The pH-rate constant profile for the reaction (3) at 37°C.

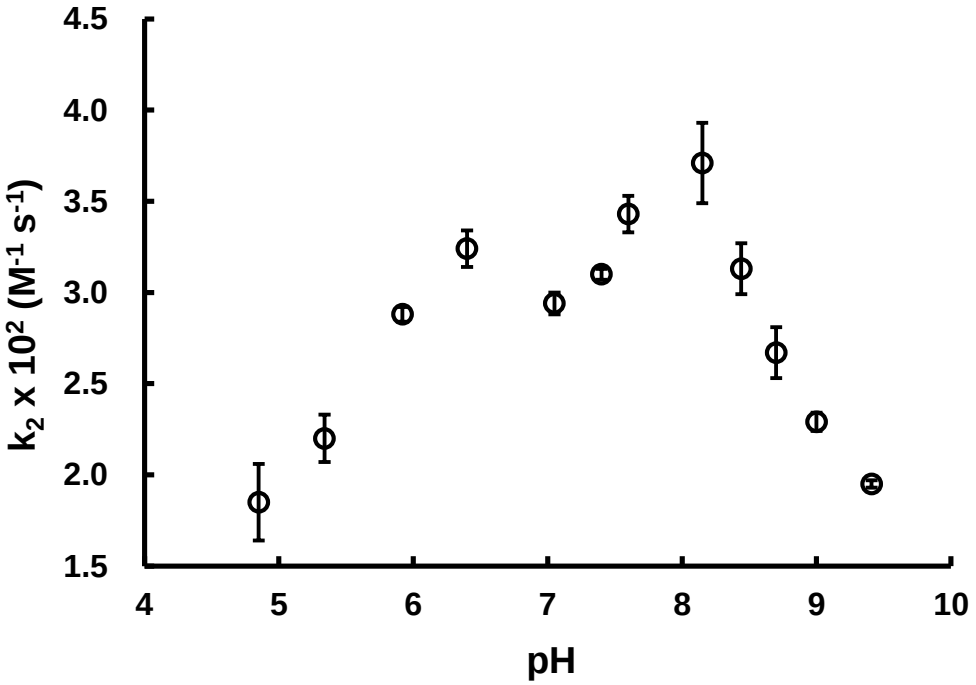

Table 1. Second order rate constants for the reaction (6)

pH	$k_2 \times 10^2$ ($M^{-1} s^{-1}$)
4.85	1.85 ± 0.21
5.34	2.20 ± 0.13
5.92	2.88 ± 0.04
6.40	3.24 ± 0.10
7.05	2.94 ± 0.06
7.40	3.10 ± 0.03
7.60	3.43 ± 0.10
8.15	3.71 ± 0.22
8.44	3.13 ± 0.14
8.70	2.67 ± 0.14
9.00	2.29 ± 0.05
9.41	1.95 ± 0.02

Chapter 2

Comparison of Contrast Agents for Atherosclerosis Imaging Using Cultured Macrophages: Fluorodeoxyglucose versus Ultrasmall Superparamagnetic Iron Oxide

Abstract

Various non-invasive imaging methods have been developed to evaluate atherosclerotic plaques. Among them, fluorodeoxyglucose-positron emission tomography (FDG-PET) and magnetic resonance imaging with ultrasmall superparamagnetic iron oxide particles (USPIO-MRI) have been used to quantify plaque inflammation. Both methods are based on the property that FDG and USPIO are efficiently taken up by macrophages in atherosclerotic lesions. Differently polarized macrophages have been reported to have different characteristics, which are involved in the pathological development of atherosclerosis. M1 polarized macrophages are considered as the more proatherogenic phenotype than M2 polarized macrophages. However, little is known regarding the association between macrophage polarization and FDG/USPIO accumulation. In this study, I investigated intracellular FDG and USPIO accumulation in M1 and M2 polarized macrophages. THP-1 macrophages were differentiated into M1 and M2 polarized macrophages. Under optimal glucose conditions, the ^{3}H-labeled FDG uptake in M1 and M2 polarized macrophages was investigated. Then intracellular USPIO uptake by M1 and M2 macrophages was investigated. As results of these experiments, it was found that M1 polarization results in increased intracellular accumulation of FDG compared to M2 polarization. To elucidate the mechanism by which FDG was preferentially accumulated in M1 macrophages, mRNA expressions of glucose transporters (GLUTs) and hexokinases (HKs), which have pivotal roles in glucose uptake, as well as glucose-6-phosphatase (G6Pase), which catalyzes the reverse reaction of HKs, were examined. In M1 macrophages, GLUT-1, GLUT-3, HK-1, and HK-2 were upregulated and G6Pase was downregulated. In contrast to FDG, M1 polarization resulted in decreased intracellular accumulation of USPIO. It was found that scavenger receptor A (SR-A) and CD11b, which are involved in USPIO binding/uptake, were

significantly downregulated by M1 polarization. In conclusion, compared to M2, proatherogenic M1 macrophages preferentially accumulated FDG but not USPIO, suggesting that FDG-PET is a useful method for the detection of proinflammatory M1 macrophages.

Introduction

The rupture of an atherosclerotic plaque heralds many cardiovascular complications such as myocardial and cerebral infarctions. Macrophage infiltration plays an important role in the development of vulnerable plaques. Fluorodeoxyglucose-positron emission tomography (^{18}F-FDG-PET) has been reported to be a promising tool for identifying vulnerable atherosclerotic plaques, because their detection depends on the extent of macrophage infiltration into the atherosclerotic lesions (Tawakol A et al., 2006; Ogawa M et al., 2004; Zhang Z et al., 2006). To date, some clinical trials have been conducted to examine the usefulness of ^{18}F-FDG-PET for evaluating atherosclerosis (Tawakol A et al., 2006; Tahara N et al., 2009). Furthermore, magnetic resonance imaging with ultrasmall superparamagnetic iron oxide particles (USPIO-MRI) that is also efficiently taken up by macrophages in the atherosclerotic lesion (Trivedi RA et al., 2006; Tang TY et al., 2009) is used to quantify atherosclerotic plaques (Tang TY et al., 2009). Recently, macrophages have been considered as heterogeneous cells, which can be differently polarized in atherosclerotic plaques (Khallou-Laschet J et al., 2010; Feig JE et al., 2011c; Bouhlel MA et al., 2007). Classically activated M1 macrophages promote the destabilization of atherosclerotic plaques, whereas alternatively activated M2 macrophages stimulate reparative processes, leading to stabilization of atherosclerotic plaques (Mantovani A et al., 2009). Therefore, effective detection of M1 macrophages may help to predict cardiovascular events with greater accuracy. However, the type of macrophages that can be detected by FDG-PET and USPIO-MRI and the effect of macrophage polarization on FDG and USPIO accumulation are still unclear.

I report here the relationship between the macrophage polarization and imaging probe uptake to the cells. I first investigated the association between macrophage polarization and FDG/USPIO accumulation using human THP-1 macrophages. Then, to

elucidate the molecular mechanism of FDG/USPIO accumulation in polarized macrophages, I analyzed the expression of genes responsible for FDG uptake and metabolism and USPIO uptake and iron export.

Materials and Methods

Cell Culture and Chemicals

Human THP-1 cells were obtained from Dainippon Sumitomo Pharma (Osaka, Japan). Cell culture media were purchased from Life Technologies (California, USA). Fetal bovine serum (FBS) was obtained from Thermo Fisher Scientific (Massachusetts, USA). Phorbol 12-myristate 13-acetate (PMA) was obtained from WAKO pure chemicals (Osaka, Japan). Lipopolysaccharides (LPS) from *Escherichia coli* O111: B4 was obtained from Sigma-Aldrich (Saint Louis, USA). Recombinant human interferon-γ (IFNγ), human interleukin (IL)-4, and human IL-13 were obtained from R&D Systems (Minneapolis, USA). [5,6-^{3}H]-2-Fluoro-2-deoxy-D-glucose (^{3}H-FDG) was obtained from American Radiolabeled Chemicals (Saint Louis, USA). USPIO coated with alkali-treated dextran (average particle size, 28 nm) was custom synthesized by Meito Sangyo (Nagoya, Japan).

Differentiation of THP-1 Cells into Macrophages and Polarization

THP-1 cells were cultured in RPMI1640 supplemented with 10% heat-inactivated FBS, 100 U/mL penicillin and 100 μg/mL streptomycin. THP-1 cells (seeded at 2×10^5 cells/cm^2) were differentiated into macrophages using 320 nM PMA and polarized according to the method of Tjiu *et al.* with some modifications (Tjiu JW et al., 2009). For M1 polarization, cells were treated with PMA for 6 h, and then cultured with PMA plus LPS (10 ng/mL) and IFNγ (20 ng/mL) for another 42 h. For M2 polarization, cells were treated with PMA for 6 h, and then cultured with PMA plus IL-4 (20 ng/mL) and IL-13 (20 ng/mL) for another 42 h. I also developed control macrophages, which received no stimuli, that were differentiated from THP-1 cells by incubation with PMA for 48 h. To evaluate the appropriate induction of polarization, I measured an M1 marker gene, inducible nitric oxide synthase (*iNOS*), and an M2 marker gene, mannose receptor C type 1 (*MRC1*).

^{3}H-FDG Study

Polarized macrophages were rinsed and then precultured in RPMI1640 containing 1 mM glucose at 37°C for 1 h. After the media were replaced with fresh media containing 1 mM glucose and ^{3}H-FDG (3.7 kBq/well), cells were cultured for another 3 h. Cells were washed twice with pre-chilled saline containing 25 mM 4-(2-hydroxyethyl)-1-piperazineethanesulfonic acid (HEPES), 1 mM $CaCl_2$, and 1 mM $MgCl_2$, and were dissolved with 0.1% sodium dodecyl sulfate/0.1 M NaOH aqueous solution. The radioactivities of culture media and cell lysates were measured using a liquid scintillation counter (Accu FLEX LSC 7400; Hitachi Aloka Medical, Ltd., Tokyo, Japan). Cellular protein concentration was measured using the DC Protein Assay Kit (Bio-Rad, California, USA). ^{3}H-FDG accumulation was expressed as radioactivities in cell lysate per milligram of cell protein.

USPIO Study

Macrophages were incubated with USPIO (400 μg Fe/mL) for the last 16 h of the 2-day treatment with polarizing stimulus at 37°C in 5% CO_2. The cells were washed twice with pre-chilled saline containing 25 mM HEPES, 1 mM $CaCl_2$, and 1 mM $MgCl_2$ and were dissolved with 0.5% Triton X-100 aqueous solution. Iron contents of cell lysates were measured using the Iron Assay Kit (BioChain, California, USA). Cellular protein concentration was measured using the DC Protein Assay Kit. The USPIO accumulation was expressed as cellular iron content per milligram of cell protein.

Gene Expression Analysis of Polarized Macrophages

Cellular total RNA was extracted using the RNeasy mini kit (QIAGEN, Hilden, Germany) and converted into cDNA using the High Capacity cDNA Reverse Transcription

Kit (Life Technologies, California, USA). Gene expression was analyzed using the 7900HT Fast Real-Time PCR System (Life Technologies, California, USA) with the TaqMan® Universal Master Mix II (Life Technologies, California, USA) and primer-probe sets of TaqMan Gene Expression Assays (Life Technologies, California, USA) for the following genes: iNOS (Hs00167248_m1), MRC1 (Hs00267207_m1), scavenger receptor A (SR-A; Hs00234012_m1), glucose transporter (GLUT)-1 (Hs00892681_m1), GLUT-3 (Hs00359840_m1), hexokinase1 (HK1; Hs00175976_m1), hexokinase2 (HK2; Hs00606086_m1), glucose-6-phosphatase (G6Pase; Hs00292720_m1), CD11b (Hs00355885_m1), CD36 (Hs00354519_m1), ferroportin 1 (Fpn1; Hs00205888_m1), and ferritin light chain (FTL; Hs00830226_gH). β-Actin (Hs99999903_m1) was used as an endogenous control gene. Relative mRNA expression was calculated using the ΔΔCT method.

Animals

All animal experimental procedures were performed according to the guidelines of the Takeda Experimental Animal Care and Use Committee. Male apolipoprotein E knockout mice ($ApoE^{-/-}$, C57BL/6J) fed high-fat diet (D12451, Research Diet, New Brunswick, USA) for 25 weeks starting at the age of 10 weeks.

Autoradiography and Oil Red O Staining

ApoE knockout mice fed high-fat diet were anaesthetized with sodium thiobutabarbital (120 mg/kg i.p.) and then intravenously injected with ^{14}C-FDG (280 kBq/mouse). The animals were kept without food O/N before injections of the radiotracers until sacrifice. Three hours after ^{14}C-FDG injections, mice were sacrificed under anesthesia and whole aorta were dissected. Excised aortas were longitudinally opened and exposed to a BAS-III imaging plate (FujiFilm, Tokyo, Japan) at -30°C for 2 days. The signals were detected by autoradiography using a FLA-7000 (FujiFilm). Following

autoradiography, the whole aortas were fixed with 10% formalin and then stained with oil red O.

Gene Expression Analysis of Atherosclerotic Plaques

ApoE knockout mice fed high-fat diet were sacrificed under anesthesia with sodium pentobarbital (55 mg/kg, i.p.) and the whole aortas were dissected after saline perfusion. The plaques in the arch and abdominal aorta were picked away and subjected to total RNA extraction. The mRNA expression was analyzed by real-time PCR method with the primer-probe sets of TaqMan Gene Expression Assays for the following genes: iNOS (Mm01309902_m1), IL-1β (Mm00434228_m1), CCR7 (Mm01301785_m1), MRC1 (Mm01329362_m1), CD68 (Mm03047343_m1), β-actin (Mm00607939_s1). β-actin was used as the internal standard gene. The relative expression level was calculated by ΔΔCT methods.

Statistics

Data are presented as mean ± SD. Statistical analyses were performed using SAS software (version 8.2; SAS Institute, Inc., Cary, NC). Either Tukey's parametric multiple comparison test or Steel–Dwass's nonparametric multiple comparison test (Bartlett's test; $P < 0.05$) was used for comparisons among the three different macrophage types, namely, M1, M2, and control macrophages. P values of < 0.05 were considered statistically significant.

Results

Macrophage Polarization

Macrophages treated with IFNγ/LPS showed significant upregulation of iNOS (Fig. 3A) ($P < 0.05$), whereas those treated with IL-4/IL-13 showed significant upregulation of MRC1 (Fig. 3B) ($P < 0.05$). The M1 marker genes CCR7 and IL-1β were also significantly upregulated in macrophages treated with IFNγ/LPS, and the M2 marker gene IL-1ra was significantly upregulated in macrophages treated with IL-4/IL-13 (data not shown). Hence, I used these macrophages as for M1 polarization and M2 polarization for the following experiments.

^{3}H-FDG Accumulation in M1 and M2 Macrophages

To study accumulation of FDG in macrophages, I first optimized the glucose concentration in the medium, since FDG-PET signals decrease if blood glucose levels exceed 200 mg/dL. In a preliminary study using a medium containing a high glucose concentration of 200 mg/dL, FDG accumulation in macrophages was markedly reduced (data not shown). In a low glucose medium of 1.8 mg/dL (approx. 0.1 mM), I observed that cells were damaged (data not shown). Therefore, I added glucose at 1 mM to the medium, so as to be sufficient to detect FDG accumulation without damaging the cells. M1 macrophages showed a 2.6-fold increased uptake of ^{3}H-FDG compared to M2 macrophages (Fig. 4) ($P < 0.01$).

Expression of Glucose Metabolism-Related Genes in Macrophages

I measured the mRNA expression of glucose metabolism-related genes to elucidate the mechanism by which FDG was preferentially taken up by M1 macrophages. I found that GLUT-1 and GLUT-3, which are major isoforms of a glucose transporter in

macrophages (Fu Y et al., 2004; Ahmed N et al., 1997), were significantly upregulated in M1 macrophages compared to M2 macrophages (Fig. 5) ($P < 0.01$ and $P < 0.01$, respectively). HK1 and HK2, which catalyze the intracellular phosphorylation of glucose into glucose-6-phosphate, were also significantly upregulated in M1 macrophages compared to M2 macrophages (Fig. 5) ($P < 0.01$ and $P < 0.01$, respectively). However, the expression of G6Pase, which is an enzyme that catalyzes the reverse reaction of hexokinases, was significantly downregulated in M1 macrophages compared to M2 macrophages (Fig. 5) ($P < 0.01$). These results suggest that the increase of FDG accumulation in M1 macrophages was caused by the upregulation of GLUT and HK genes, as well as the downregulation of G6Pase gene.

USPIO Accumulation in M1 and M2 Macrophages

Previous USPIO accumulation studies have used macrophages treated with USPIO in concentrations ranging from 50 to 500 μg Fe/mL and in time periods lasting 1 to 72 h (Lunov O et al., 2011; Müller K et al., 2008; Yancy AD et al., 2005; Raynal I et al., 2004). On the basis of our preliminary study findings, macrophages were incubated with USPIO (400 μg Fe/mL) for the last 16 h of the 2-day treatment with polarizing stimulus at 37°C in 5% CO_2. USPIO accumulation in the cells increased linearly with both USPIO concentration and incubation time. In contrast to FDG, USPIO accumulation in M2 macrophages was 1.4-fold higher than that in M1 macrophages (Fig. 6) ($P < 0.01$).

Expression of USPIO Uptake- and Iron Export-Related Genes in Macrophages

To elucidate the mechanism by which USPIO was preferentially taken up by M2 macrophages compared to M1 macrophages, I measured the mRNA expression of SR-A and CD11b (Lunov O et al., 2011; von Zur Muhlen C et al., 2007). Both SR-A and CD11b were significantly upregulated in M2 macrophages compared to M1 macrophages (Fig. 7)

($P < 0.01$ and $P < 0.01$, respectively). Considering that other scavenger receptors may contribute to the uptake of USPIO, I measured the expression of CD36, another major scavenger receptor. As shown in Fig. 7, CD36 was also upregulated in M2 macrophages. The expression of Fpn1, the major iron exporter in mammalian cells (Donovan A et al., 2005), was also significantly upregulated in M2 macrophages compared to M1 macrophages (Fig. 7) ($P < 0.01$). There was no significant difference in the expression of FTL, which is responsible for intracellular iron storage (Torti FM et al., 2002), between M1 macrophages and M2 macrophages (Fig. 7).

^{14}C-FDG Accumulation in Murine Atherosclerotic Plaques

Next, I qualitatively investigated ^{14}C-FDG accumulation *ex vivo* in atherosclerotic plaques of ApoE knockout mice fed high fat diet as murine model of atherosclerosis. Oil red O staining revealed that atherosclerotic plaques were rich in both arch and abdominal aorta in this atherosclerosis model. Notwithstanding, signals of ^{14}C-FDG accumulation were observed stronger in the abdominal plaques compared to plaques in the aortic arch in *en face* autoradiography of the whole aorta of ^{14}C-FDG injected ApoE KO mice (Fig. 8).

Expression of Polarized Macrophage Marker in Murine Atherosclerotic Plaques

To investigate the relationship between ^{14}C-FDG accumulation and macrophage polarization in atherosclerotic plaques in this mouse model, the expression level of marker genes of macrophage polarization was subsequently measured. The expression of M1 marker genes, such as iNOS, IL-1β, CCR7, was upregulated in the abdominal plaques where more ^{14}C-FDG was accumulated than the aortic arch ones (Fig. 9). Conversely, the expression of M2 marker gene MRC1 was significantly upregulated in the aortic arch plaques (Fig. 9) ($P < 0.05$). The expression of macrophage marker gene CD68 was not

different significantly between the aortic arch plaques and the abdominal one (Fig. 9).

Discussion

FDG-PET and USPIO-MRI have been clinically used to quantify atherosclerotic plaques, because both FDG and USPIO are efficiently taken up by macrophages in atherosclerotic lesions. Recently, macrophages in varying polarized states have been reported to have different characteristics that are involved in the pathological development of atherosclerosis (Khallou-Laschet J et al., 2010; Mantovani A et al., 2009). In this study, I compared the ability of differently polarized macrophages to take up FDG and USPIO using human THP-1 macrophages. I showed that FDG was taken up preferentially by M1 macrophages, whereas USPIO was taken up by M2 macrophages.

The preferential uptake of FDG by M1 macrophages led to the hypothesis that M1 and M2 differed in the expression of the glucose uptake-related molecules because FDG is taken up by cells in a manner analogous to glucose. I observed that the mRNA expression of GLUT-1 and GLUT-3 was upregulated in M1 macrophages. Kim *et al.* also reported that the mRNA expression of GLUT-1 was upregulated and intracellular FDG accumulation increased in mouse RAW264.7 macrophages stimulated by LPS (Kim C et al., 2009). In addition, I showed that the mRNA expression of HK1 and HK2, which are major hexokinase isoforms, was upregulated, whereas the mRNA expression of G6Pase was downregulated in M1 macrophages. FDG is taken up into cells via glucose transporters and then phosphorylated by hexokinases to FDG-6-phosphate (FDG6P) in a mechanism similar to glucose. FDG6P is retained inside the cell, such that it can neither follow the process of glycolysis nor easily pass through the plasma membrane. If G6Pase, the catalyst of the reverse reaction of hexokinase, converts FDG6P into FDG, FDG can theoretically diffuse out of cells via glucose transporters. The present study suggests that the regulation of gene expression of key molecules involved in glucose uptake contributed to the increase in intracellular FDG accumulation in M1 macrophages. In particular, the

increased intracellular FDG uptake via glucose transporters, the phosphorylation of FDG by hexokinases, and the decrease in dephosphorylation of FDG6P by G6Pase contributed to the increase of FDG uptake in M1 macrophages. On the other hand, inconsistent with our observation, Folco *et al.* reported that inflammatory stimulation did not increase the glucose uptake in human primary monocytes (Folco EJ et al., 2011). They used IFNγ or a combination of IFNγ, TNFα and IL-1β as inflammatory stimulation, whereas I adopted a classical M1 stimulation for characterizing typical phenotypes of M1 macrophages. I need to consider a more relevant stimulation to atherosclerosis in the future experiments.

Small iron oxide particles (SPIO) and USPIO have been used clinically as superparamagnetic MRI contrast agents. These iron oxide particles are efficiently taken up by macrophages. A range of molecules is considered to be involved in SPIO/USPIO uptake and iron export. Lunov *et al.* identified the clathrin-mediated SR-A dependent endocytosis as a major pathway of USPIO uptake in peripheral blood monocyte-derived macrophages (Lunov O et al., 2011). Muhlen *et al.* showed that USPIO uptake was inhibited by treatment with anti-CD11b antibody in PMA-stimulated human peripheral blood monocytes (von Zur Muhlen C et al., 2007). In the present study, I determined that both SR-A and CD11b were significantly upregulated in M2 macrophages, which might contribute to the increase in USPIO uptake by M2 macrophages (Fig 7). Gu *et al.* reported that internalized USPIO in mouse macrophages was degraded in lysosomes and free iron was released into intracellular iron pools (Gu J et al., 2011). Fpn1 is known to have an important role in the export of iron from cells (Donovan A et al., 2005). I observed that Fpn1 was also upregulated in M2 macrophages compared to M1 macrophages (Fig. 7), consistent with the previous report (Recalcati S et al., 2010). In the present study, I observed statistically significant increase of USPIO uptake in M2 macrophages compared to M1 macrophages, but the difference was relatively small, in spite of the marked induction of genes related to uptake of USPIO. The upregulation of Fpn1 could cause the

reduction of the cellular iron levels, which might attenuate the accumulation of USPIO in M2 macrophages. Taken together, accumulation of cellular USPIO was higher in M2 macrophages than in M1 macrophages, most likely as a result of the balance of transcriptional regulation of genes related to uptake and export of USPIO. In the present study, there were no difference in USPIO accumulation between M2 macrophages and control ones (Fig. 6), suggesting the difficulty of visualizing only M2 macrophages in distinction from non-polarized macrophage by USPIO. Recently, it has been reported that the status of macrophages polarization in atherosclerotic plaques was dramatically changed in the progression and regression process of atherosclerosis using experimental murine model (Feig JE et al., 2011c; Feig JE et al., 2011p). In addition, a substantial number of macrophages was polarized in those lesions. Therefore, USPIO should be able to light-up the mainly M2-lesion, although I need to pay attention to the false-positive results. In contrast to our findings, Rogers *et al.* reported that not only Th2 cytokine IL-4 but also Th1 cytokine IFNγ increased SPIO uptake in mouse J774A.1 macrophages (Rogers WJ et al., 2005). However, differing experimental conditions including cell type and polarization methods might explain these discrepancies. Rogers *et al.* used IFNγ and IL-4 alone as Th1 and Th2 cytokines, respectively, whereas I used IFNγ in addition to LPS and IL-4 plus IL-13 as M1-polarizing and M2-polarizing stimuli, respectively. In this study, I investigated the USPIO uptake with a 16 h incubation to obtain the reasonably enough amount of intracellular USPIO for quantitative analysis, while the incubation time was 3 h for FDG. The exposure time might affect the uptake of FDG and USPIO in M1 and M2 polarized macrophages. Cell viability also should be another important factor to evaluate the cellar uptake. In this study, at least, the cell damage was not observed morphologically. Further investigation about exposure time and cell viability should be needed for the precise analysis.

The ultimate purpose of atherosclerosis imaging, and the detection of vulnerable

rupture-prone plaques in particular, is the accurate prediction of cardiovascular events. Recently, studies have suggested that the quality rather than quantity of macrophages is critical in the evolution of vulnerable plaques (Hartung D et al., 2007; Matter CM et al., 2006; Jarrett BR et al., 2010). M1 macrophages play a key role in the development of atherosclerosis, which is mediated by production of proinflammatory cytokines and/or reactive nitrogen oxides, whereas M2 macrophages have antiatherogenic properties mediated by the production of anti-inflammatory cytokines and the suppression of proinflammatory signaling (Gordon S et al., 2005; Wolfs IM et al., 2011). However, the contribution of these differently polarized macrophages to vulnerable plaque formation, potentially resulting in plaque rupture has not yet been fully understood. For example, Mauriello *et al*. recently reported that M2 but not M1 macrophages were present in the fibrous cap near the rupture site in the human carotid artery, suggesting that M2 macrophages might also modulate the process of plaque rupture (Mauriello A, et al., 2011). Although further investigations regarding the roles of M1 and M2 macrophages in atherosclerotic lesions are needed, it is clear that macrophage polarization affects plaque diagnosis and prognosis. *Ex vivo* study, stronger signals were observed in abdominal plaques compared to plaques in the aortic arch in en face autoradiography of the whole aorta of ^{14}C-FDG injected ApoE KO mice (Fig. 8). The M1 markers iNOS, IL-1β, CCR7 were upregulated in the abdominal plaques, while the M2 marker MRC1 was upregulated in the aortic arch plaques (Fig. 9). These results suggest that ^{18}F-FDG-PET should dominantly visualize the M1 macrophage infiltrated area though there is the limitation that number of macrophages in each atherosclerotic plaque is not able to be normalized by molecular biological technique. With respect to this consideration, an additional investigation on quantification of macrophage content in atherosclerotic plaques by an immunohistochemical method will lead to a more precise result. Some reports have suggested that ^{18}F-FDG-PET may be useful to monitor the therapeutic

effects of drugs (Fayad ZA et al., 2011; Tahara N et al., 2006; Ogawa M et al., 2006), and some of the drugs are reported to affect the polarization of macrophages (Bouhlel MA et al., 2007; Feig JE et al., 2011c; Aki K et al., 2010; Fujita E et al, 2010). Because therapies which reduce M1 macrophages are garnering more attention, it becomes increasingly important to select appropriate imaging methods that accurately detect plaque development.

In conclusion, the present study provides in vitro evidence that ^{18}F-FDG PET preferentially detects proinflammatory M1 macrophages, whereas USPIO MR imaging preferentially detects anti-inflammatory M2 macrophages. Although further *in vivo* investigations are needed, ^{18}F-FDG PET imaging should be useful in the detection of proinflammatory M1 macrophages.

Figures

Figure 3. Gene expression of M1 and M2 markers in human THP-1 macrophages treated with each polarizing factor: (A) iNOS as M1 marker, (B) MRC1 as M2 marker. Data are presented as mean ± SD (N = 6). *$P < 0.05$ compared between M1 and M2; #$P < 0.05$ compared to No stimuli by Steel-Dwass test.

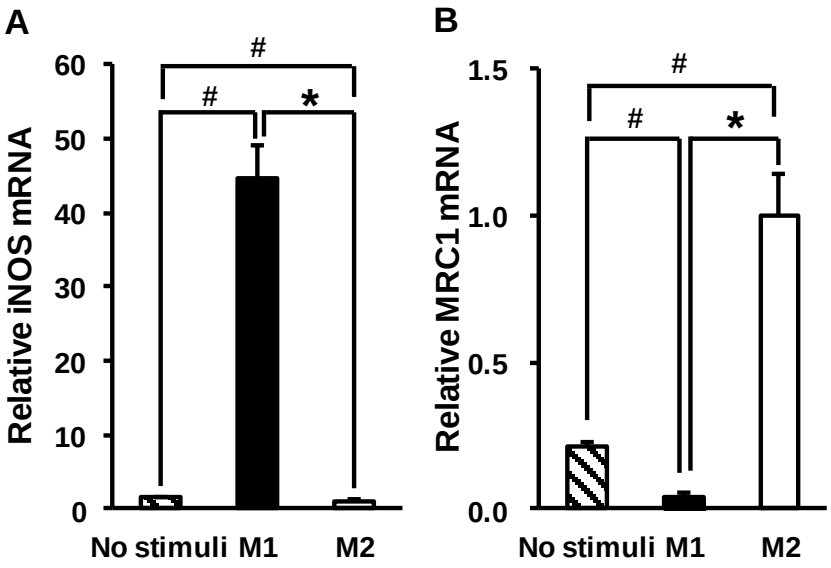

Figure 4. Intracellular [^{3}H]FDG accumulation in human THP-1 macrophages. Data are presented as mean ± SD (N = 6). $^{**}P < 0.01$ compared between M1 and M2; $^{\#\#}P < 0.01$ compared to No stimuli by Tukey test.

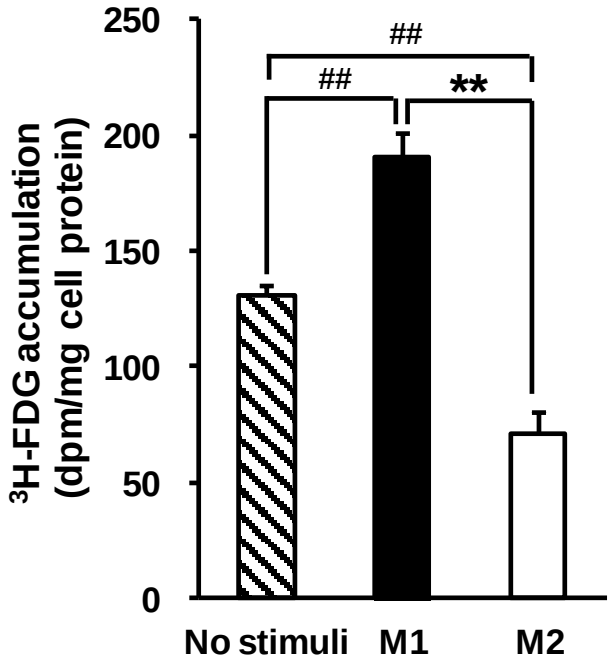

Figure 5. Expression of glucose metabolism-related genes in human THP-1 macrophages: (A) GLUT-1, (B) GLUT-3, (C) HK1, (D) HK2, (E) G6Pase. Data are presented as mean ± SD (N = 6). $^{**}P < 0.01$ compared between M1 and M2; $^{\#\#}P < 0.01$ compared to No stimuli by Tukey test.

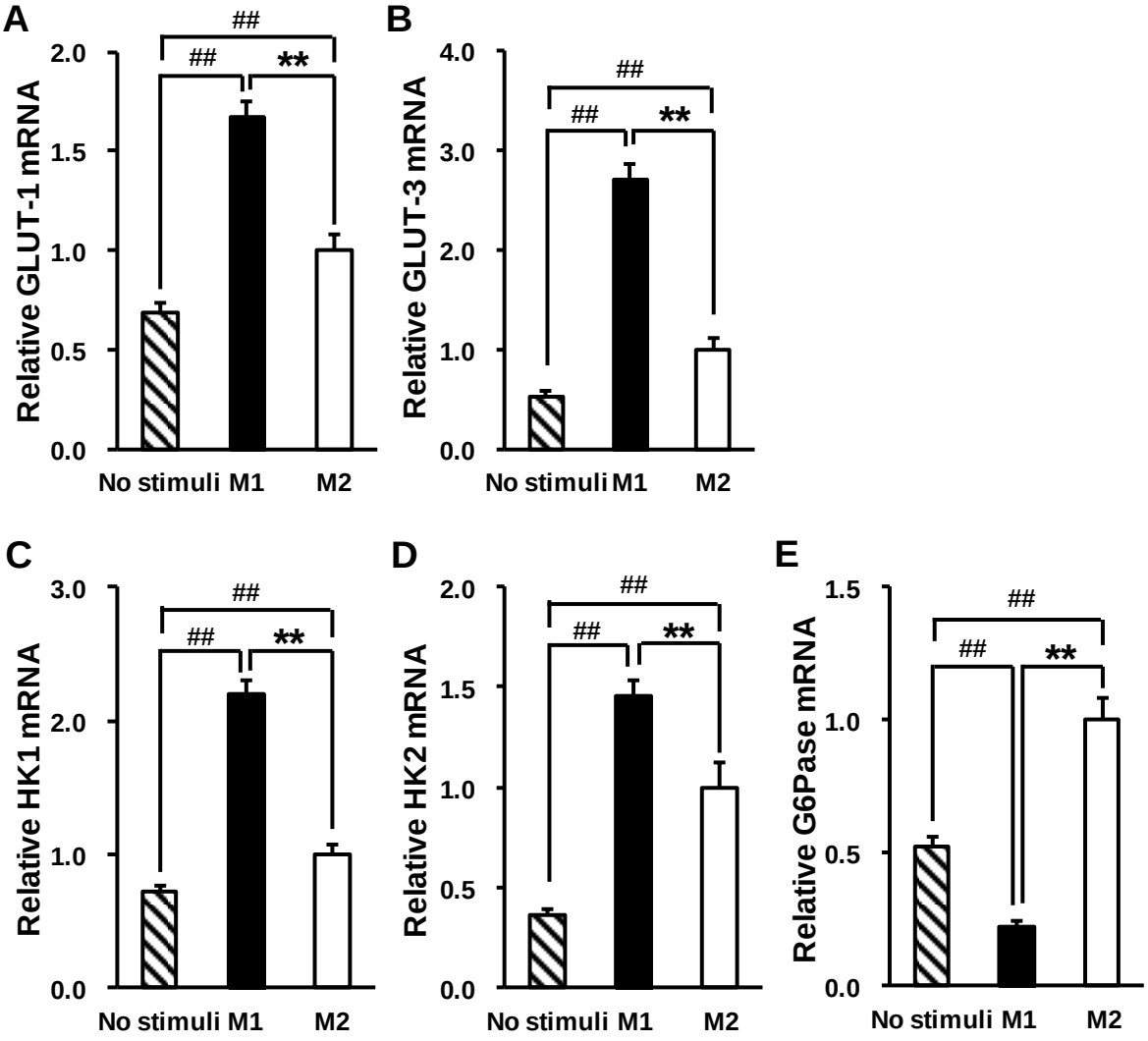

Figure 6. Intracellular USPIO accumulation in human THP-1 macrophages. Data are presented as mean ± SD (N = 6). $^{**}P < 0.01$ compared between M1 and M2; $^{\#\#}P < 0.01$ compared to No stimuli by Tukey test.

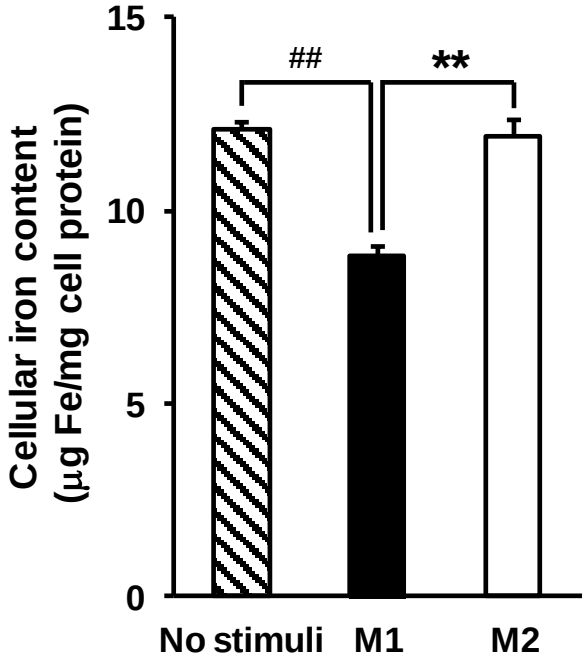

Figure 7. Expression of USPIO uptake- and iron export-related genes in human THP-1 macrophages: (A) SR-A, (B) CD11b, (C) CD36, (D) Fpn1, (E) FTL. Data are presented as mean ± SD (N = 6). *$P < 0.05$, **$P < 0.01$ compared between M1 and M2; #$P < 0.05$, ##$P < 0.01$ compared to No stimuli by Tukey test of Steel-Dwass test.

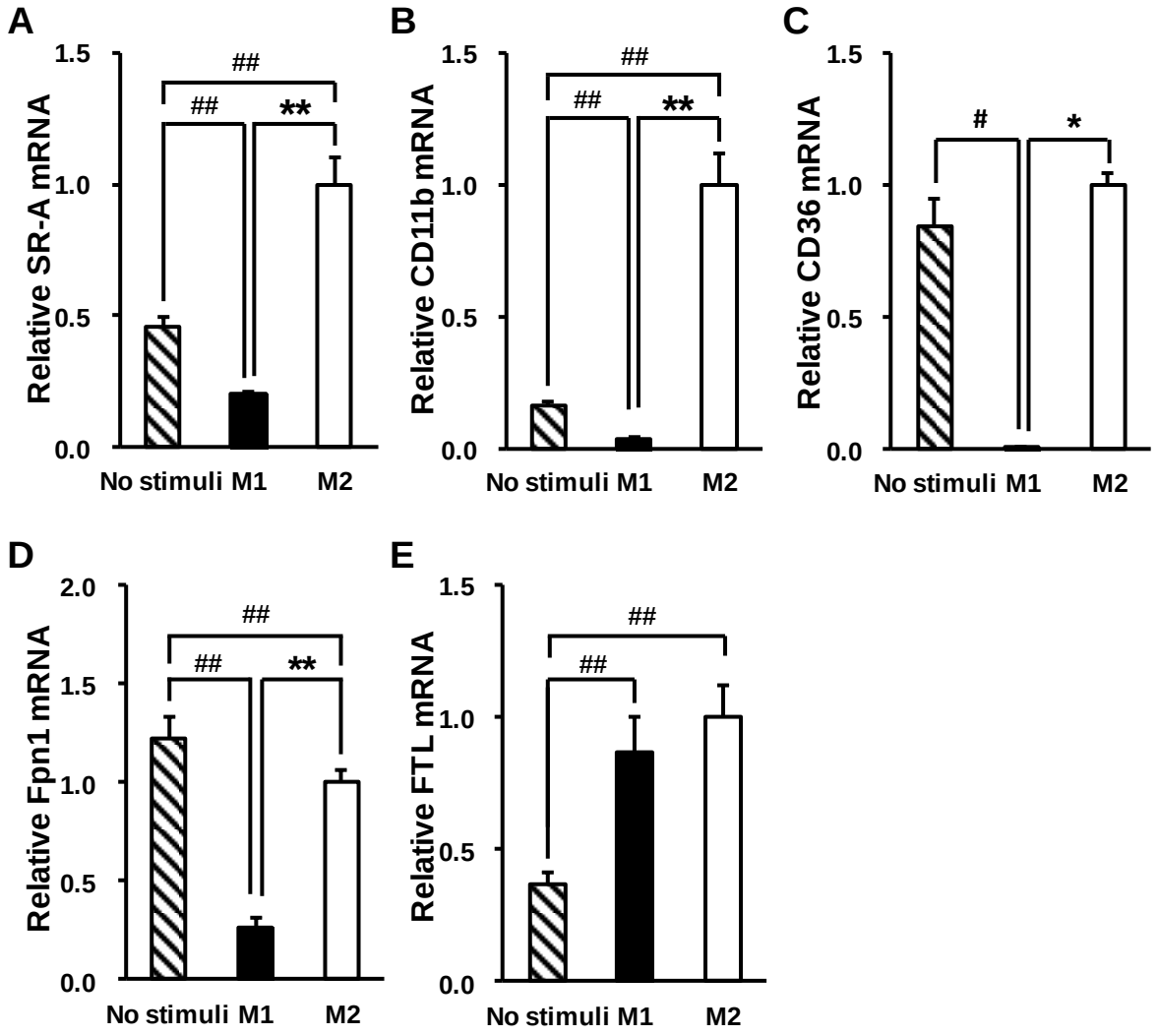

Figure 8. Autoradiography (A) and corresponding oil red O staining (B) in mouse aortas after 14C-FDG injections. The aortas with the same numbers indicated in the figure were obtained from the same animals.

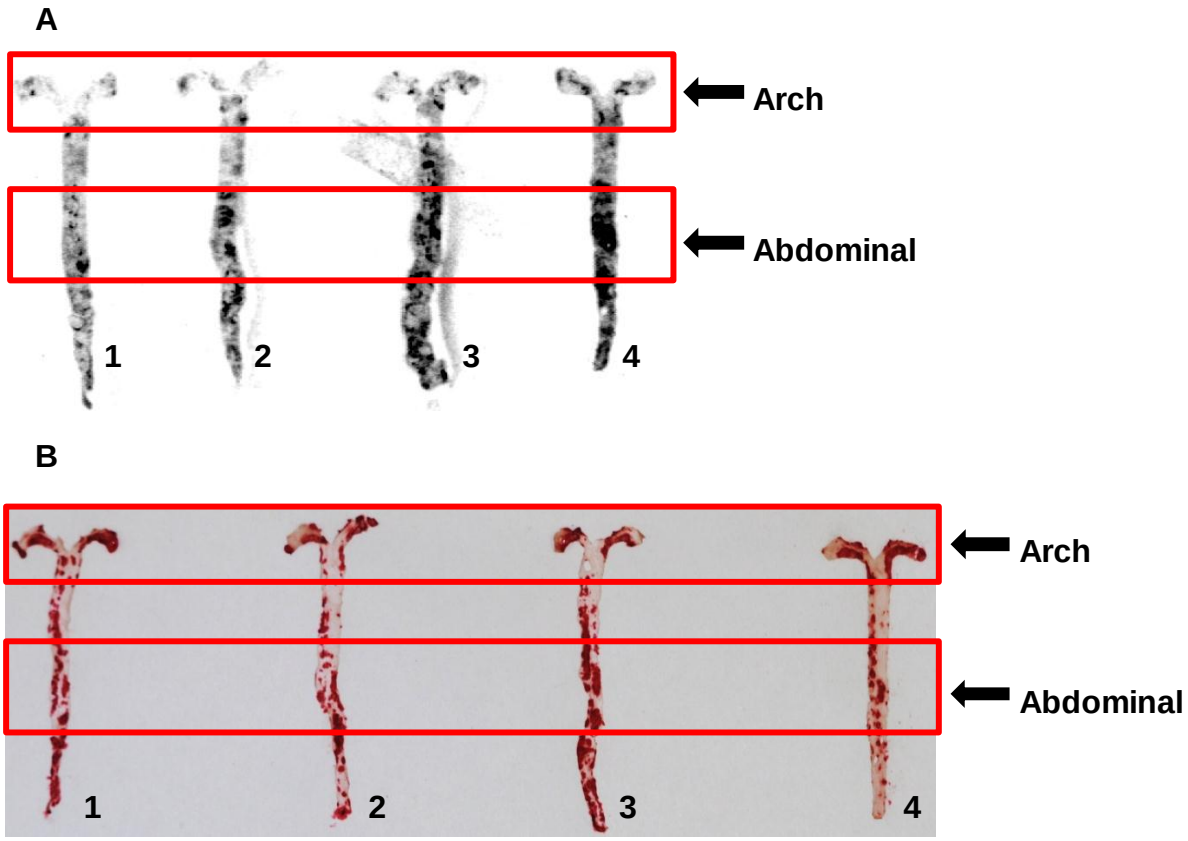

Figure 9. Gene expression of M1 (iNOS, IL-1β, CCR7) , M2 (MRC1) and macrophage (CD68) markers in the aortic arch (white bar) and abdominal (black bar) plaques from ApoE knockout mice. Data are presented as mean ± SD (N = 6). *P < 0.05 by Student *t* test.

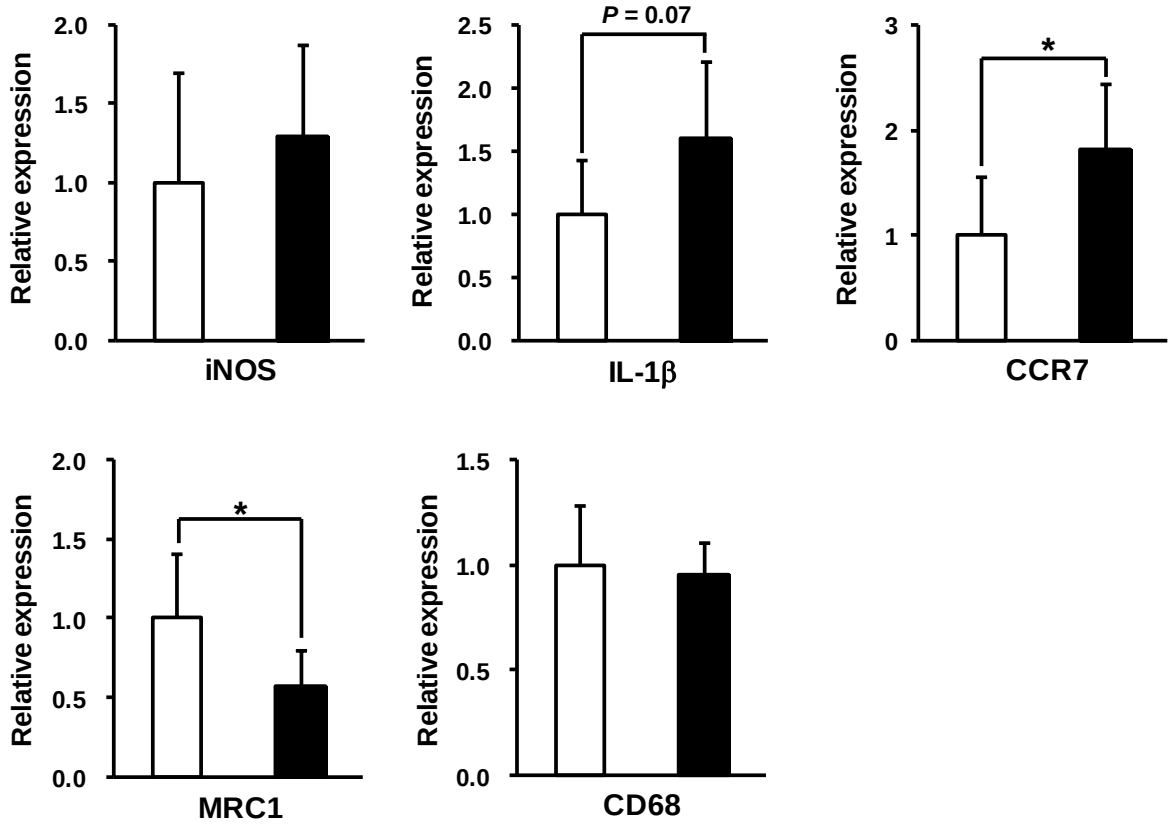

General Discussion

In this thesis, I investigated the usefulness of metabolically stable compounds, such as S-nitrosocysteine, FDG, and USPIO, as tools for various biological approaches. In Chapter 1, the decomposition kinetics of S-nitrosocysteine, one of endogenous S-nitrosothiols, were investigated in order to understand its usefulness as a sustainable NO donor. I discussed the physiological role and usefulness of S-nitrosocysteine and the future perspective to its clinical translation, led by my study. In Chapter 2, M1/M2-polarized macrophages were characterized using two types of chemical probes, FDG and USPIO, which were metabolized through different pathways. Biological readout of the imaging using FDG and USPIO in atherosclerosis was discussed based on kinetic research of these compounds in the different type of macrophages. I also discussed the results from the point of view of translational research.

In chapter 1, in order to investigate whether S-nitrosothiols could work as an NO donor in a body, its decomposition rate was evaluated in the presence of cysteine for mimicking a physiological condition. For this study, I used S-nitrosocysteine which is structurally the simplest S-nitrosothiol presented in cells and blood. S-nitrosocysteine was physiologically produced via S-nitrosation of cysteine by nitrous acid that is produced from NO in the presence of oxygen (reaction 1), or via transnitrosation reaction between an S-nitrosothiol and cysteine (reaction 3). The present study indicated that a half-life of S-nitrosocysteine was approx. 75 min, much longer half-life than NO, suggesting that S-nitrosocysteine could function as a NO reservoir in physiological conditions. It has been reported that high-molecular-weight S-nitrosothiols such as S-nitrosoalbumin and S-nitrosohemoglobin showed a more sustainable property, compared to

low-molecular-weight S-nitrosothiols, such as S-nitrosocysteine and S-nitrosoglutathione. For example, the half-life of S-nitrosoalbumin in human plasma *in vitro* was 5.5 hours determined by GC-MS (Tsikas D et al., 1999). Because NO itself is a labile free radical with the biological half-life of several seconds, Cys-34 residue of serum albumin is nitrosylated to form long lived S-nitrosoalbumin, which may act as a reservoir of NO in blood (Simon DI et al., 1993; Shcarftein JS et al., 1994). In physiological conditions, NO is supposed to be stored as stable high-molecular-weight S-nitrosothiols by a rapid transnitrosation reaction, whose nitroso group is then transferred into low–molecular-weight S-nitrosothiols, particularly S-nitrosocysteine. S-nitrosocysteine crosses the plasma membrane into intracellular targets via the L-type amino acid transporters (Li S et al., 2005), and then is degraded to release NO both enzymatically and non-enzymatically and functions as an intracellular NO donor. On the other hand, NO is oxidized to nitrous acid in the presence of oxygen, and transported in blood as a form of nitrite ion. It has been reported that protonation of nitrite ion produces nitrosonium ion (NO^+), which reacts with thiols in blood, and is converted into S-nitrosothiols (Grossi L et al., 2002). S-nitrosothiols also have a physiological important role in this recycling pathway of NO. It is indicated that S-nitrosothiols including S-nitrosocysteine can become a tool compound to elucidate various physiological function of NO, because they are produced endogenously and have a sufficient stability to function *in vivo*. Actually, S-nitrosothiols are used widely for the research of NO especially in cardiovascular system. Previous reports (Hogg N, 2000; Richardson G et al., 2002) and the present result indicate that the some S-nitrosothiols are useful as sustainable

NO-generating tools for the NO research, and overcome the problem related to extreme, highly unstable property of NO molecule. Moreover, S-nitrosoglutathion, one of S-nitrosothiols, has also been used as an NO donor for treatment of patients in small clinical trials (Molloy J et al., 1998; Salas E et al., 1998; Rassaf T et al., 2002). However, S-nitrosothiols have not yet been launched in the market, because their decomposition rate is unpredictable because various factors, such as trace amounts of copper ions, enzymatic degradation, and transnitrosation with other thiols, affects their decomposition (Richardson G et al, 2002). Although the clinical use of S-nitrosothiols is currently challenging, other approaches to increase NO by eNOS activation are clinically available at present. There are some launched drugs which increase eNOS activity. For example, 3-hydroxy-3-methylglutaryl–coenzyme A (HMG-CoA) reductase inhibitors as anti-hyperlipidemic drugs, angiotensin-converting enzyme (ACE) inhibitors as anti-hypertensive drugs, and prostacyclin analogues as drugs for pulmonary hypertension and peripheral arterial disease increase NO production based on upregulation of eNOS at mRNA level. These drugs improve vascular endothelial functions due to vasodilatory effect and inhibitory effect of platelet aggregation via NO elevation. However, other approaches to increase NO are still desired. Further researches on the mechanism of the decomposition of S-nitrosothiols are required for their clinical usage as NO donors. The present research might help to understand this mechanism.

In chapter 2, I studied the difference on the characteristics of M1/M2-polarized macrophages by use of two types of contrast agent, FDG and USPIO. FDG, which is an analogue of glucose, is taken up by cells via GLUTs and phosphorylated to

FDG-6-phosphate by HKs to the same extent as glucose. However, FDG-6-phosphate is unable to be metabolized further in the glycolytic pathway and remains within the cells differently from glucose-6-phosphate. Therefore, glucose uptake can be stably monitored using this stable contrast agent (Sheikine Y and Akram K, 2010). Conversely, USPIO is iron oxide nanoparticles coated with dextran with a mean diameter of approx. 30 nm, similar to that of low density lipoprotein (LDL) (15 to 25 nm). Macrophages take up proatherogenic lipoproteins as oxidized LDL through scavenger receptors and are converted into foam cells. It has reported that USPIO particles are taken up by macrophages via the scavenger receptor-mediated endocytosis (von Zur Muhlen C et al., 2007; Lunov O et al., 2011), and metabolized via the lysosomal pathway (Schulze E et al., 1995). In vascular vessels, the inflammatory response induced by M1 macrophages within the atherosclerotic plaque stimulates macrophages both to undergo apoptosis, which contributes to necrotic core formation, and to secrete matrix metalloproteinases (MMPs), which degrade the fibrous cap, and then promotes plaque instability (Tiwari RL et al., 2008; Moore KJ et al., 2011). The present study clearly demonstrated that inflammatory M1 macrophages preferentially accumulated FDG than USPIO, due to upregulation of both glucose uptake and glucose phosphorylation in M1 macrophages. It is important to translate *in vitro* observation into *in vivo* situation, especially clinical one. In the *ex vivo* study of mouse model of atherosclerosis, signals of ^{14}C-FDG accumulation were observed stronger in the abdominal plaques compared to plaques in the aortic arch in *en face* autoradiography of the whole aorta of ^{14}C-FDG injected ApoE KO mice. The expression of M1 marker genes, such as iNOS, IL-1β, CCR7, was upregulated in the abdominal plaques

where more ^{14}C-FDG was accumulated than the aortic arch ones, suggesting that FDG accumulation was enhanced in an atherosclerotic plaque which was increased the ratio of M1-polarized inflammatory macrophages. I selected high fat diet-fed ApoE KO mice as a mouse model of atherosclerosis because they were known to spontaneously develop unstable atherosclerotic plaques whose disruption caused cardiovascular events (Jackson CL et al., 2007; Matoba T et al., 2013). However, some researchers pointed out the species difference between mice and humans regarding the complexity of their atherosclerotic lesion (Schwartz SM et al., 2007). For extrapolating the present study into clinical atherosclerosis, further investigations are needed about histopathological analysis of the mouse model using in this study, including quantitative determination of infiltrating macrophages in atherosclerotic lesion. However, the present results are consistent with clinical observations, because it has been reported that the pharmaceutical intervention of anti-atherosclerotic drugs, such as pioglitazone, polarized macrophages in human atherosclerotic lesion to M2 (Bouhlel MA et al., 2007), and decreased FDG accumulation in atherosclerotic lesion by FDG-PET study via attenuation of atherosclerotic plaque inflammation (Mizoguchi M et al., 2011). The selection of an appropriate probe to detect inflammatory M1 macrophages leads to the improvement of a predictive probability for cardiovascular events, because inflammatory macrophages contribute to promote the destabilization of atherosclerotic plaques. The present study strongly suggests that FDG can be more useful than USPIO as an imaging probe that detects the inflammatory M1 macrophages.

The metabolically stable compounds in the body are useful for not only investigating

various life phenomena, but also applying to our life such as clinical diagnosis and therapy. In addition, it is essential for life sciences to explore new metabolically stable chemical probes designed by modification of endogenous molecules.

Acknowledgements

I would like to express my sincere gratitude towards my supervisor, Professor Osamu Numata, University of Tsukuba, for his pertinent indications and valuable discussions through my doctoral program.

I especially would like to express my deepest appreciation to my supervisors, Dr. Tomoyuki Nishimoto, Takeda Pharmaceutical Company, Limited, and Professor Ken Fujimori, University of Tsukuba, for their elaborated guidance, considerable encouragement and invaluable discussion that make my research of great achievement and my study life unforgettable.

I also would like to express my appreciation to my collaborators, Dr. Mikako Ogawa and Professor Yasuhiro Magata, Hamamatsu University School of Medicine, for helpful suggestion and discussions.

I also would like to express my appreciation to my supervisors, Dr. Masaki Hosoya, Dr. Masakuni Noda, and Dr. Seigo Izumo, Takeda Pharmaceutical Company Limited, for providing me this precious study opportunity as a Ph.D student.

I am very grateful to my colleagues in Takeda Pharmaceutical Company Limited, for their valuable cooperation and discussion.

References

Abeles, R. H., Frey, P. A, Jencks, W. P., (1992). Biochemistry. *Jones and Bartlett*, Boston.

Ahmed, N., Kansara, M., Berridge, M. V. (1997). Acute regulation of glucose transport in a monocyte-macrophage cell line: Glut-3 affinity for glucose is enhanced during the respiratory burst. *Biochem J* **327**, 369-75.

Aki, K., Shimizu, A., Masuda, Y., Kuwahara, N., Arai, T., Ishikawa, A., Fujita, E., Mii, A., Natori, Y., Fukunaga, Y., Fukuda, Y. (2010). ANG II receptor blockade enhances anti-inflammatory macrophages in anti-glomerular basement membrane glomerulonephritis. *Am J Physiol Renal Physiol* **298**, F870-82.

Allen, B. W., Piantadosi, C. A. (2006). How do red blood cells cause hypoxic vasodilation? The SNO-hemoglobin paradigm. *Am J Physiol Heart Circ Physiol* **291**, H1507-12.

Angelo, M., Singel, D. J., Stamler, J. S. (2006). An S-nitrosothiol (SNO) synthase function of hemoglobin that utilizes nitrite as a substrate. *Proc Natl Acad Sci USA* **103**,8366-71.

Arnelle, D. R., Stamler, J. S. (1995). NO^+, NO, and NO^- donation by S-nitrosothiols: implications for regulation of physiological functions by S-nitrosylation and acceleration of disulfide formation. *Arch Biochem Biophys* **318**, 279-85.

Askew, S. C., Barnett, D. J., McAninly, J., Williams, D. L. H. (1995). Catalysis by Cu^{2+} of nitric oxide release from S-nitrosothiols (RSNO). *J Chem Soc Perkin Trans 2*, 741-5.

Barnett, D. J., McAninly, J., Williams, D. L. H. (1994). Transnitrosation between nitrosothiols and thiols. *J Chem Soc Perkin Trans 2*, 1131-3.

Barnett, D. J., Rios, A., Williams, D. L. H. (1995). NO-group transfer (transnitrosation) betweenS. *J Chem Soc Perkin Trans 2*, 1279–82.

Bouhlel, M. A., Derudas, B., Rigamonti, E., Dièvart, R., Brozek, J., Haulon, S., Zawadzki,

C., Jude, B., Torpier, G., Marx, N., Staels, B., Chinetti-Gbaguidi, G. (2007). PPARgamma activation primes human monocytes into alternative M2 macrophages with anti-inflammatory properties. *Cell Metab* **6**, 137-43.

Bredt, D. S., Snyder, S. H. (1994). Nitric oxide: a physiologic messenger molecule. *Annu Rev Biochem* **63**, 175-95.

Cook, P. F., Cleland, W. W. (2007). Enzyme kinetics and mechanism, *Garland Science,* New York.

Craven, P. A., DeRubertis, F. R. (1978). Restoration of the responsiveness of purified guanylate cyclase to nitrosoguanidine, nitric oxide, and related activators by heme and hemeproteins. Evidence for involvement of the paramagnetic nitrosyl-heme complex in enzyme activation. *J Biol Chem* **253**, 8433-43.

Crawford, J. H., White, C. R., Patel, R. P. (2003). Vasoactivity of S-nitrosohemoglobin: role of oxygen, heme, and NO oxidation states. *Blood* **101**, 4408-15.

Derbyshire, E. R., Marletta, M. A. (2009). Biochemistry of soluble guanylate cyclase. *Handb. Exp. Pharmacol.* **191**, 17-31.

Donovan, A., Lima, C. A., Pinkus, J. L., Pinkus, G. S., Zon, L. I., Robine, S., Andrews, N. C. (2005). The iron exporter ferroportin/Slc40a1 is essential for iron homeostasis. *Cell Metab* **1**, 191-200.

Fayad, Z. A., Mani, V., Woodward, M., Kallend, D., Abt, M., Burgess, T., Fuster, V., Ballantyne, C. M., Stein, E. A., Tardif, J. C., Rudd, J. H., Farkouh, M. E., Tawakol, A. (2011). Safety and efficacy of dalcetrapib on atherosclerotic disease using novel non-invasive multimodality imaging (dal-PLAQUE): a randomised clinical trial. *Lancet*

378, 1547-59.

Feelisch, M., te Poel, M., Zamora, R., Deussen, A., Moncada, S. (1994). Understanding the controversy over the identity of EDRF. *Nature* **368**, 62-5.

Feig, J. E., Parathath, S., Rong, J. X., Mick, S. L., Vengrenyuk, Y., Grauer, L., Young, S. G., Fisher, E. A. (2011). Reversal of hyperlipidemia with a genetic switch favorably affects the content and inflammatory state of macrophages in atherosclerotic plaques. *Circulation*, **123**, 989-98.

Feig, J. E., Rong, J. X., Shamir, R., Sanson, M., Vengrenyuk, Y., Liu, J., Rayner, K., Moore, K., Garabedian, M., Fisher, E. A. (2011). HDL promotes rapid atherosclerosis regression in mice and alters inflammatory properties of plaque monocyte-derived cells. *Proc Natl Acad Sci USA* **108**, 7166-71.

Fu, Y., Maianu, L., Melbert, B. R., Garvey, W. T. (2004). Facilitative glucose transporter gene expression in human lymphocytes, monocytes, and macrophages: a role for GLUT isoforms 1, 3, and 5 in the immune response and foam cell formation. *Blood Cells Mol Dis* **32**, 182-90.

Fujita, E., Shimizu, A., Masuda, Y., Kuwahara, N., Arai, T., Nagasaka, S., Aki, K., Mii, A., Natori, Y., Iino, Y., Katayama, Y., Fukuda, Y. (2010). Statin attenuates experimental anti-glomerular basement membrane glomerulonephritis together with the augmentation of alternatively activated macrophages. *Am J Pathol* **177**, 1143-54.

Folco, E. J., Sheikine, Y., Rocha, V. Z., Christen, T., Shvartz, E., Sukhova, G. K., Di Carli, M. F., Libby, P. (2011). Hypoxia but not inflammation augments glucose uptake in human macrophages: Implications for imaging atherosclerosis with 18fluorine-labeled

2-deoxy-D-glucose positron emission tomography. *J Am Coll Cardiol* **58**, 603-14.

Fukuto, J. M., Hobbs, A. J., Ignarro, L. J. (1993). Conversion of nitroxyl (HNO) to nitric oxide (NO) in biological systems: the role of physiological oxidants and relevance to the biological activity of HNO. *Biochem Biophys Res Commun* **196**, 707-13.

Furchgott, R. F. (1988). Mechanisms of Vasodilation. Raven Press, New York, 401–14.

Gordon, S., Taylor, P. R. (2005). Monocyte and macrophage heterogeneity. *Nat Rev Immunol* **5**, 953-964.

Girard, P., Potier, P. (1993). NO, thiols and disulfides. *FEBS Lett* **320**, 7-8.

Goldstein S., Czapski, G. (1996). Mechanism of the Nitrosation of Thiols and Amines by Oxygenated ·NO Solutions: the Nature of the Nitrosating Intermediates. *J Am Chem Soc* **118**, 3419–25.

Gratzel, M., Taniguchi, S., Henglein, A. (1970). Pulse radiolytic study of NO oxidation and of the equilibrium N_2O_3. dbr.NO + NO_2 in aqueous solution. *Ber Bunsen-Ges Phys Chem* **74**, 488-92

Gross, W. L., Bak, M. I., Ingwall, J. S., Arstall, M. A., Smith, T. W., Balligand, J. L., Kelly, R. A. (1996). Nitric oxide inhibits creatine kinase and regulates rat heart contractile reserve. *Proc Natl Acad Sci USA* **93**, 5604-9.

Grossi, L, Montevecchi, P. C. (2002). S-nitrosocysteine and cystine from reaction of cysteine with nitrous acid. A kinetic investigation. *J Org Chem* **67**, 8625-30.

Gu, J., Xu, H., Han, Y., Dai, W., Hao, W., Wang, C., Gu, N., Xu, H., Cao, J. (2011). The internalization pathway, metabolic fate and biological effect of superparamagnetic iron oxide nanoparticles in the macrophage-like RAW264.7 cell. *Sci China Life Sci* **54**,

793-805.

Hajjar, D. P., Lander, H. M., Pearce, S. F. A., Upmacis, R. K., Pomerantz, K. B. (1995). Nitric oxide enhances prostaglandin-H synthase-1 activity by a heme-independent mechanism: Evidence implicating nitrosothiols. *J Am Chem Soc* **117**, 3340–6.

Hartung, D., Schäfers, M., Fujimoto, S., Levkau, B., Narula, N., Kopka, K., Virmani, R., Reutelingsperger, C., Hofstra, L., Kolodgie, F. D., Petrov, A., Narula, J. (2007). Targeting of matrix metalloproteinase activation for noninvasive detection of vulnerable atherosclerotic lesions. *Eur J Nucl Med Mol Imaging* **34**, S1-8.

Hogg N. (2000). Biological chemistry and clinical potential of S-nitrosothiols. *Free Radic Biol Med* **28**, 1478-86.

Hu, T. M., Chou, T. C. (2006). The kinetics of thiol-mediated decomposition of S-nitrosothiols. *AAPS J* **8**, E485-92.

Ignarro, L. J. (1989). Biological actions and properties of endothelium-derived nitric oxide formed and released from artery and vein. *Circ Res* **65**, 1-21.

Ignarro, L. J., Byrns, R. E., Wood, K. S. (1987). Endothelium-dependent modulation of cGMP levels and intrinsic smooth muscle tone in isolated bovine intrapulmonary artery and vein. *Circ Res* **60**, 82-92.

Jackson, C. L., Bennett, M. R., Biessen, E. A., Johnson, J. L., Krams, R. (2007). Assessment of unstable atherosclerosis in mice. *Arterioscler Thromb Vasc Biol* **27**, 714-20.

Jarrett, B. R., Correa, C., Ma, K. L., Louie, A. Y. (2010). *In vivo* mapping of vascular inflammation using multimodal imaging. *PLoS One* **5**, e13254.

Jia, L., Bonaventura, C., Bonaventura, J., Stamler, J. S. (1996). S-nitrosohaemoglobin: a dynamic activity of blood involved in vascular control. *Nature* **380**, 221-6.

John McAninly, J., Williams, D. L. H., Askew, S. C., Butler, A. R., Russell, C. (1993). Metal ion catalysis in nitrosothiol (RSNO) decomposition. *J Chem Soc Chem Commun*, 1758-9.

Khallou-Laschet, J., Varthaman, A., Fornasa, G., Compain, C., Gaston, A. T., Clement, M., Dussiot, M., Levillain O, Graff-Dubois S, Nicoletti A, Caligiuri G. (2010). Macrophage plasticity in experimental atherosclerosis. *PLoS One* **5**, e8852.

Kharitonov, V. G., Sundquist, A. R., Sharma, V. S. (1995). Kinetics of nitrosation of thiols by nitric oxide in the presence of oxygen. *J Biol Chem* **270**, 28158-64.

Kim C, Kim S. (2009). Taurine chloramine inhibits LPS-induced glucose uptake and glucose transporter 1 expression in RAW 264.7 macropages. *Adv Exp Med Biol* **643**, 473-80.

Klopman, G. (1974). Chemical Reactivity and Reaction Paths. John Wiley & Sons, New York, 55-166

Levy, J. H. (1996). The human inflammatory response. *J Cardiovasc Pharmacol* **27** Suppl 1, S31-7.

Li, S., Whorton, A. R. (2005). Identification of stereoselective transporters for S-nitroso-L-cysteine: role of LAT1 and LAT2 in biological activity of S-nitrosothiols. *J Biol Chem*. **280**, 20102-10.

Lunov, O., Zablotskii, V., Syrovets, T., Röcker, C., Tron, K., Nienhaus, G. U., Simmet, T. (2011). Modeling receptor-mediated endocytosis of polymer-functionalized iron oxide

nanoparticles by human macrophages. *Biomaterials* **32**, 547-55.

Mantovani, A., Garlanda, C., Locati, M. (2009). Macrophage diversity and polarization in atherosclerosis: a question of balance. *Arterioscler Thromb Vasc Biol* **29**, 1419-23.

Marletta, M. A. (1993). Nitric oxide synthase structure and mechanism. *J Biol Chem* **268**, 12231-12234.

Martin, B. R. (1987). Metabolic Regulation: Molecular Approach. *Blackwell Scientific*, Oxford, UK.

Matoba, T., Sato, K., Egashira, K. (2013). Mouse models of plaque rupture. *Curr Opin Lipidol* **24**, 419-25.

Matter, C. M., Wyss, M. T., Meier, P., Späth, N., von Lukowicz, T., Lohmann, C., Weber, B., Ramirez de Molina, A., Lacal, J. C., Ametamey, S. M., von Schulthess, G. K., Lüscher, T. F., Kaufmann, P. A., Buck, A. (2006). 18F-choline images murine atherosclerotic plaques ex vivo. *Arterioscler Thromb Vasc Biol* **26**, 584-9.

Mauriello, A., Servadei, F., Sangiorgi, G., Anemona, L., Giacobbi, E., Liotti, D., Spagnoli, L. G. (2011). Asymptomatic carotid plaque rupture with unexpected thrombosis over a non-canonical vulnerable lesion. *Atherosclerosis* **218**, 356-62.

McGilvery, R. H. (1983). Biochemistry: A Functional Approach, 3rd ed. *Saunders*, Philadelphia.

Mizoguchi, M., Tahara, N., Tahara, A., Nitta, Y., Kodama, N., Oba, T., Mawatari, K., Yasukawa, H., Kaida, H., Ishibashi, M., Hayabuchi, N., Harada, H., Ikeda, H., Yamagishi, S., Imaizumi, T. (2011). Pioglitazone attenuates atherosclerotic plaque inflammation in patients with impaired glucose tolerance or diabetes a prospective, randomized,

comparator-controlled study using serial FDG PET/CT imaging study of carotid artery and ascending aorta. *JACC Cardiovasc Imaging* **4**, 1110-8.

Mohr, S., Stamler, J. S., Brüne, B. (1994). Mechanism of covalent modification of glyceraldehyde-3-phosphate dehydrogenase at its active site thiol by nitric oxide, peroxynitrite and related nitrosating agents. *FEBS Lett* **348**, 223-7.

Molloy, J., Martin, J. F., Baskerville, P. A., Fraser, S. C. A., Markus, H. S. (1998). S-nitrosoglutathione reduces the rate of embolization in humans. *Circulation* **98**, 1372–5.

Moore, K. J., Tabas, I. (2011). Macrophages in the pathogenesis of atherosclerosis. *Cell* **145**, 341-55.

Müller, K., Skepper, J. N., Tang, T. Y., Graves, M. J., Patterson, A. J., Corot, C., Lancelot, E., Thompson, P. W., Brown, A. P., Gillard, J. H. (2008). Atorvastatin and uptake of ultrasmall superparamagnetic iron oxide nanoparticles (Ferumoxtran-10) in human monocyte-macrophages: implications for magnetic resonance imaging. *Biomaterials* **29**, 2656-62.

Newsholme, E. A., Start, C. (1973). Regulation in Metabolism. *Wiley*, New York.

Oae, S., Fukushima, D., Kim, Y. H. (1977). Novel method of activating thiols by their conversion into thionitrites with dinitrogen tetroxide. *J Chem Soc Chem Commun* , 407b-408.

Oae, S., Asai, N., Fujimori, K. (1978). The kinetics and mechanism of the aminolysis of phenethyl nitrite. *J Chem Soc Perkin Trans 2*, 1124-1130.

Ogawa, M., Ishino, S., Mukai, T., Asano, D., Teramoto, N., Watabe, H., Kudomi, N., Shiomi, M., Magata, Y., Iida, H., Saji, H. (2004). (18)F-FDG accumulation in

atherosclerotic plaques: immunohistochemical and PET imaging study. *J Nucl Med* **45**, 1245-50.

Ogawa, M., Magata, Y., Kato, T., Hatano, K., Ishino, S., Mukai, T., Shiomi, M., Ito, K., Saji, H. (2006). Application of 18F-FDG PET for monitoring the therapeutic effect of antiinflammatory drugs on stabilization of vulnerable atherosclerotic plaques. *J Nucl Med* **47**, 1845-50.

Osborn, E. A., Jaffer, F. A. (2013). The advancing clinical impact of molecular imaging in CVD. *JACC Cardiovasc Imaging* **6**, 1327-41.

Palmer RM, Ferrige AG, Moncada S. (1987). Nitric oxide release accounts for the biological activity of endothelium-derived relaxing factor. *Nature* **327**, 524-6.

Park, J. W. (1988). Reaction of S-nitrosoglutathione with sulfhydryl groups in protein. *Biochem Biophys Res Commun* **152**, 916-20.

Rand, M. J., Li, C. G. (1995). Nitric oxide as a neurotransmitter in peripheral nerves: nature of transmitter and mechanism of transmission. *Annu Rev Physiol* **57**, 659-82.

Rassaf, T., Kleinbongard, P., Preik, M., Dejam, A., Gharini, P., Lauer, T., Erckenbrecht, J., Duschin, A., Schulz, R., Heusch, G., Feelisch, M., Kelm, M. (2002). Plasma nitrosothiols contribute to the systemic vasodilator effects of intravenously applied NO: experimental and clinical Study on the fate of NO in human blood. *Circ Res* **91**, 470-7.

Raynal, I., Prigent, P., Peyramaure, S., Najid, A., Rebuzzi, C., Corot, C. (2004). Macrophage endocytosis of superparamagnetic iron oxide nanoparticles: mechanisms and comparison of ferumoxides and ferumoxtran-10. *Invest Radiol* **39**, 56-63.

Recalcati, S., Locati, M., Marini, A., Santambrogio, P., Zaninotto, F., De Pizzol, M.,

Zammataro, L., Girelli, D., Cairo, G. (2010). Differential regulation of iron homeostasis during human macrophage polarized activation. *Eur J Immunol* **40**, 824-35.

Richardson, G., Benjamin, N. (2002). Potential therapeutic uses for S-nitrosothiols. *Clin Sci* **102**, 99-105.

Rogers, W. J., Basu, P. (2005). Factors regulating macrophage endocytosis of nanoparticles: implications for targeted magnetic resonance plaque imaging. *Atherosclerosis* **178**, 67-73.

Salas, E., Langford, E. J., Marrinan, M. T., Martin, J. F., Moncada, S., Debelder, A. J. (1998). S-nitrosoglutathione inhibits platelet activation and deposition in coronary artery saphenous vein grafts in vitro and *in vivo*. *Heart* **80**, 146–50.

Scharfstein, J. S., Keaney, J. F., Jr, Slivka, A., Welch, G. N., Vita, J. A., Stamler, J. S., Loscalzo, J. (1994). *In vivo* transfer of nitric oxide between a plasma protein-bound reservoir and low molecular weight thiols. *J Clin Invest* **94**, 1432-9.

Schechter, A. N., Gladwin, M. T. (2003). Hemoglobin and the paracrine and endocrine functions of nitric oxide. *N Engl J Med* **348**, 1483-5.

Schoenheimer, R. (1946). The dynamic state of body constituents. *Harvard Univ Press*, Cambridge. x + 78.

Schulz, G. E., Schirmer, R. H. (1979). Principles of protein structure. *Springer Verlag*, New York. 1-314.

Schulze, E., Ferrucci, J. T., Poss, K., Lapointe, L., Bogdanova, A., Weissleder, R. (1995). Cellular uptake and trafficking of a prototypical magnetic iron oxide label in vitro. *Invest Radiol* **30**, 604–610.

Schwartz, S. M., Galis, Z. S., Rosenfeld, M. E., Falk, E. (2007). Plaque rupture in humans and mice. *Arterioscler Thromb Vasc Biol* **27**, 705-13.

Sheikine, Y., Akram, K. (2010). FDG-PET imaging of atherosclerosis: Do we know what we see? *Atherosclerosis* **211**, 371-80.

Simon, D. I., Stamler, J. S., Jaraki, O., Keaney, J. F., Osborne, J. A., Francis, S. A., Singel, D. J., Loscalzo, J. (1993). Antiplatelet properties of protein S-nitrosothiols derived from nitric oxide and endothelium-derived relaxing factor. *Arterioscler Thromb* **13**, 791-9.

Smith, T. A. (1998). FDG uptake, tumour characteristics and response to therapy: a review. *Nucl Med Commun* **19**, 97-105.

Stamler, J. S. (1994). Redox signaling: nitrosylation and related target interactions of nitric oxide. *Cell* **78**, 931-6.

Stamler, J. S., Jaraki, O., Osborne, J., Simon, D. I., Keaney, J., Vita, J., Singel, D., Valeri, C. R., Loscalzo, J. (1992). Nitric oxide circulates in mammalian plasma primarily as an S-nitroso adduct of serum albumin. *Proc Natl Acad Sci USA* **89**, 7674-7.

Stamler, J. S., Simon, D. I., Osborne, J. A., Mullins, M. E., Jaraki, O., Michel, T., Singel, D. J., Loscalzo, J. (1992). S-nitrosylation of proteins with nitric oxide: synthesis and characterization of biologically active compounds. *Proc Natl Acad Sci USA* **89**, 444-8.

Stamler, J. S., Singel, D. J., Loscalzo, J. (1992). Biochemistry of nitric oxide and its redox-activated forms. *Science* **258**, 1898-902.

Tahara, N., Imaizumi, T., Virmani, R., Narula, J. (2009) Clinical feasibility of molecular imaging of plaque inflammation in atherosclerosis. *J Nucl Med* **50**, 331-4.

Tang, T. Y., Howarth, S. P., Miller, S. R., Graves, M. J., Patterson, A. J., U-King-Im, J. M.,

Li, Z.Y., Walsh, S. R., Brown, A. P., Kirkpatrick, P. J., Warburton, E. A., Hayes, P. D., Varty, K., Boyle, J. R., Gaunt, M. E., Zalewski, A., Gillard, J. H. (2009). The ATHEROMA (Atorvastatin Therapy: Effects on Reduction of Macrophage Activity) Study. Evaluation using ultrasmall superparamagnetic iron oxide-enhanced magnetic resonance imaging in carotid disease. *J Am Coll Cardiol* **53**, 2039-50.

Tawakol, A., Migrino, R. Q., Bashian, G. G., Bedri, S., Vermylen, D., Cury, R. C., Yates, D., LaMuraglia G. M., Furie, K., Houser, S., Gewirtz, H., Muller, J. E., Brady, T. J., Fischman, A. J. (2006). *In vivo* 18F-fluorodeoxyglucose positron emission tomography imaging provides a noninvasive measure of carotid plaque inflammation in patients. *J Am Coll Cardiol* **48**, 1818-24.

Tejero, J., Basu, S., Helms, C., Hogg, N., King, S.B., Kim-Shapiro, D.B., Gladwin, M.T. (2012). Low NO concentration dependence of reductive nitrosylation reaction of hemoglobin. *J Biol Chem* **287**, 18262-74.

Tiwari, R. L., Singh, V., Barthwal, M. K. (2008). Macrophages: an elusive yet emerging therapeutic target of atherosclerosis. *Med Res Rev* **28**, 483-544.

Tjiu, J. W., Chen, J. S., Shun, C. T., Lin, S. J., Liao, Y. H., Chu, C. Y., Tsai, T. F., Chiu, H. C., Dai, Y. S., Inoue, H., Yang, P. C., Kuo, M. L., Jee, S. H. (2009). Tumor-associated macrophage-induced invasion and angiogenesis of human basal cell carcinoma cells by cyclooxygenase-2 induction. *J Invest Dermatol* **129**, 1016-25.

Trivedi, R. A., Mallawarachi, C., U-King-Im, J. M., Graves, M. J., Horsley, J., Goddard, M. J., Brown, A., Wang, L., Kirkpatrick, P. J., Brown, J., Gillard, J. H. (2006). Identifying inflamed carotid plaques using *in vivo* USPIO-enhanced MR imaging to label plaque

macrophages. *Arterioscler Thromb Vasc Biol* **26**, 1601-6.

Torti, F. M., Torti, S. V. (2002). Regulation of ferritin genes and protein. *Blood* **99**, 3505-16.

Tahara, N., Kai, H., Ishibashi, M., Nakaura, H., Kaida, H., Baba, K., Hayabuchi, N., Imaizumi, T. (2006). Simvastatin attenuates plaque inflammation: evaluation by fluorodeoxyglucose positron emission tomography. *J Am Coll Cardiol* **48**, 1825-31.

Tang, T., Howarth, S. P., Miller, S. R., Trivedi, R., Graves, M. J., King-Im, J. U., Li, Z. Y., Brown, A. P., Kirkpatrick, P. J., Gaunt, M. E., Gillard, J. H. (2006). Assessment of inflammatory burden contralateral to the symptomatic carotid stenosis using high-resolution ultrasmall, superparamagnetic iron oxide-enhanced MRI. *Stroke* **37**, 2266-70.

Tsikas, D., Sandmann, J., Rossa, S., Frölich, J. C. (1999). Measurement of S-nitrosoalbumin by gas chromatography–mass spectrometry. I. Preparation, purification, isolation, characterization and metabolism of S-[^{15}N]nitrosoalbumin in human blood in vitro. *J Chromatogr, B* **726**, 1–12.

Wanders, R. J. (2013). Peroxisomes in human health and disease: metabolic pathways, metabolite transport, interplay with other organelles and signal transduction. *Subcell Biochem* **69**, 23-44.

Wolfs, I. M., Donners, M. M., de Winther, M. P. (2011). Differentiation factors and cytokines in the atherosclerotic plaque micro-environment as a trigger for macrophage polarisation. *Thromb Haemost* **106**, 763-71.

Yancy, A. D., Olzinski, A. R., Hu, T. C., Lenhard, S. C., Aravindhan, K., Gruver, S. M., Jacobs, P. M., Willette, R. N., Jucker, B. M. (2005). Differential uptake of ferumoxtran-10

and ferumoxytol, ultrasmall superparamagnetic iron oxide contrast agents in rabbit: critical determinants of atherosclerotic plaque labeling. *J Magn Reson Imaging* **21**, 432-42.

Yoshinaga, K., Tamaki, N. (2007). Imaging myocardial metabolism. *Curr Opin Biotechnol* **18**, 52-9.

Zhang, Z., Machac, J., Helft, G., Worthley, S. G., Tang, C., Zaman, A. G., Rodriguez, O. J., Buchsbaum, M. S., Fuster, V., Badimon, J. J. (2006). Non-invasive imaging of atherosclerotic plaque macrophage in a rabbit model with F-18 FDG PET: a histopathological correlation. *BMC Nucl Med* **6**, 3.

von Zur Muhlen, C., von Elverfeldt, D., Bassler, N., Neudorfer, I., Steitz, B., Petri-Fink, A., Hofmann, H., Bode, C., Peter, K. (2007). Superparamagnetic iron oxide binding and uptake as imaged by magnetic resonance is mediated by the integrin receptor Mac-1 (CD11b/CD18): implications on imaging of atherosclerotic plaques. *Atherosclerosis* **193**, 102-11.